NASA CONTRACTOR REPORT

INFLIGHT AND GROUND-BASED SIMULATION OF HANDLING QUALITIES OF VERY LARGE AIRPLANES IN LANDING APPROACH

by Philip M. Condit, Laddie G. Kimbrel, and Robert G. Root

Prepared by
BOEING COMPANY
Seattle, Wash.
for Ames Research Center

NATIONAL AERONAUTICS AND SPACE ADMINISTRATION • WASHINGTON, D. C. • OCTOBER 1966

NASA CR-635

INFLIGHT AND GROUND-BASED SIMULATION OF HANDLING QUALITIES OF VERY LARGE AIRPLANES IN LANDING APPROACH

By Philip M. Condit, Laddie G. Kimbrel,
and Robert G. Root

Prepared under Contract No. NAS 2-3224 by
BOEING COMPANY
Seattle, Wash.

for Ames Research Center

NATIONAL AERONAUTICS AND SPACE ADMINISTRATION

For sale by the Clearinghouse for Federal Scientific and Technical Information
Springfield, Virginia 22151 – Price $2.50

FOREWORD

This report was prepared under Contract NAS2-3224 between The Boeing Company, Seattle, Washington, and the National Aeronautics and Space Administration. The NASA project monitor was Hervey C. Quigley and the NASA project pilot was Robert C. Innis.

The authors gratefully acknowledge the invaluable help of the NASA and Boeing Company personnel associated with this project.

CONTENTS

INFLIGHT AND GROUND-BASED SIMULATION OF HANDLING QUALITIES OF VERY LARGE AIRPLANES IN LANDING APPROACH

By Philip M. Condit, Laddie G. Kimbrel, and Robert G. Root

SUMMARY

A ground-based and inflight piloted simulator program was conducted utilizing the NASA-Ames moving base transport simulator, and the Boeing 367-80 variable stability airplane. The study examined several of the problem areas associated with handling qualities of large transport airplanes in the landing approach.

With lateral-directional dynamics augmented to provide satisfactory STOL handling qualities, it was found that pilot opinion was more influenced by roll response sensitivity, as measured by the roll response obtained for a given wheel input, than by total roll control power. Having selected configurations with good roll performance sensitivity, an improvement in pilot opinion was obtained with an increase in roll damping. The longitudinal evaluation indicated that pilot opinion was dependent on both pitching moment sensitivity and lift due to elevator motion.

INTRODUCTION

The next few years should see the introduction of very large, transport-category aircraft into military and civilian aviation. Inherent in these aircraft are handling qualities problems associated with inertias considerably larger than those experienced to date. It is difficult to provide these large aircraft with handling characteristics that satisfy criteria developed for small aircraft. This investigation was undertaken in order to improve the understanding of several of the important problem areas of these airplanes in the landing approach flight regime. In particular, attention was directed to the factors that define required levels of lateral and longitudinal control.

The study covered both lateral and longitudinal airplane characteristics. The lateral investigation covered control power, control sensitivity, rolling mode time constant, wheel force gradient, and control system response time. The longitudinal study examined pitch control sensitivity, lift due to control, static stability, pitch damping, and lift curve slope.

The study had two phases: a ground-based simulator study and an inflight simulation. The ground-based effort was designed to cover a wide range of variables and thus to indicate the important trends and areas for the inflight simulation. The inflight simulation served to verify the results of the ground-based tests.

This report presents the pilot ratings obtained from the lateral control and longitudinal control and stability parameters studied for the landing approach. These data were analyzed in terms of several existing handling qualities parameters as well as in terms of other parameters developed in the course of data analysis; however, no attempt was made at a comprehensive comparison with other sources or the development of definitive criteria.

NOMENCLATURE

b	wing span, ft
$\bar{c}$	mean aerodynamic cord, ft
C_D	drag coefficient
C_l	rolling moment coefficient
C_L	lift coefficient
C_m	pitching moment coefficient
C_n	yawing moment coefficient
C_Y	side force coefficient
C_{D_α}	$\partial C_D/\partial \alpha$ per radian
C_{l_β}	$\partial C_l/\partial \beta$ per radian
$C_{l_{\dot{\psi}}}$	$\partial C_l/\partial \dot{\psi}$ per radian/sec
$C_{l_{\delta_r}}$	$\partial C_l/\partial \delta_r$ per radian
$C_{l_{\dot{\phi}}}$	$\partial C_l/\partial \dot{\phi}$ per radian/sec
$C_{l_{\delta_w}}$	$\partial C_l/\partial \delta_w$ per radian
$C_{L_{\dot{\theta}}}$	$\partial C_L/\partial \dot{\theta}$ per radian /sec
C_{L_α}	$\partial C_L/\partial \alpha$ per radian
$C_{L_{\dot{\alpha}}}$	$\partial C_L/\partial \dot{\alpha}$ per radian/sec
$C_{L_{\delta_e}}$	$\partial C_L/\partial \delta_e$ per radian
C_{m_α}	$\partial C_m/\partial \alpha$ per radian

$C_{m_{\dot{\alpha}}}$	$\partial C_m/\partial \dot{\alpha}$ per radian/sec
$C_{m_{\dot{\theta}}}$	$\partial C_m/\partial \dot{\theta}$ per radian/sec
$C_{m_{\delta_e}}$	$\partial C_m/\partial \delta_e$ per radian
$C_{m_{i_H}}$	$\partial C_m/\partial i_H$ per radian
C_{n_β}	$\partial C_n/\partial \beta$ per radian
$C_{n_{\dot{\phi}}}$	$\partial C_n/\partial \dot{\phi}$ per radian/sec
$C_{n_{\dot{\psi}}}$	$\partial C_n/\partial \dot{\psi}$ per radian/sec
$C_{n_{\delta_a}}$	$\partial C_n/\partial \delta_a$ per radian
$C_{n_{\delta_r}}$	$\partial C_n/\partial \delta_r$ per radian
C_{Y_β}	$\partial C_Y/\partial \beta$ per radian
$C_{Y_{\dot{\phi}}}$	$\partial C_Y/\partial \dot{\phi}$ per radian/sec
$C_{Y_{\dot{\psi}}}$	$\partial C_Y/\partial \dot{\psi}$ per radian/sec
$C_{Y_{\delta_a}}$	$\partial C_Y/\partial \delta_a$ per radian
$C_{Y_{\delta_r}}$	$\partial C_Y/\partial \delta_r$ per radian
d	offset distance, ft
E_{in}	input, volts
E_o	output, volts
F_s	column force, pounds
F_w	wheel force, pounds
g	acceleration due to gravity, ft/sec^2
h	height above ground, ft
i_H	horizontal stabilizer angle, degrees
I_{xx}	moment of inertia about X axis, slug-ft^2
I_{yy}	moment of inertia about Y axis, slug-ft^2
I_{zz}	moment of inertia about Z axis, slug-ft^2
I_{xz}	cross product of inertia, slug-ft^2
L	roll acceleration, radians/sec^2

L_β	$\partial L/\partial \beta$ per sec^2
L_{δ_c}	$\partial \dot{\gamma}/\partial \delta_c = \frac{1}{V} \partial n_z / \partial \delta_c$ radians/sec/in.
L_α	$\frac{\partial \dot{\gamma}}{\partial \alpha} = \frac{1}{V} \frac{\partial n_z}{\partial \alpha} = C_{L_\alpha} \frac{qS}{mV}$ per sec
M	pitch acceleration, rad/sec^2
M_{δ_c}	$\partial M/\partial \delta_c$, radians/sec^2/in.
M_α	$\partial M/\partial_\alpha$ per sec^2
$M_{\dot{\theta}}$	$\partial M/\partial_{\dot{\theta}}$ per sec
mac	mean aerodynamic chord, ft
n_z	acceleration normal to flight path, ft/sec^2
q	dynamic pressure, lb/ft^2
s	Laplace operator
S	wing area, ft^2
$t_{1/2}$	time to half amplitude, sec
t_{max}	time to maximum rolling acceleration, sec
V	velocity, ft/sec, knots
α	angle of attack, radians
β	angle of sideslip, radians
δ_{ab}	spoiler angle, radians
δ_c	column displacement, inches
δ_e	elevator angle, radians
δ_r	rudder angle, radians
δ_{th}	thrust lever angle, radians
δ_w	wheel angle, degrees
$\delta_{w_{eff}}$	effective wheel angle, wheel angle for maximum rolling moment, degrees

ζ	damping ratio,
$\dot{\theta}$	pitch rate, radians/sec
$\ddot{\theta}$	pitch acceleration, radians/sec^2
γ	longitudinal flight path angle, radians
$\dot{\gamma}$	longitudinal flight path angle rate, radians/sec
τ_R	rolling mode time constant (negative inverse of the characteristic equation root), seconds
ϕ	roll angle, radians, degrees
$\dot{\phi}$	roll rate, radians/sec
$\ddot{\phi}$	roll acceleration, radians/sec^2
$\dot{\psi}$	yaw rate, radians/sec
ω_n	undamped natural frequency, radians/sec

Subscripts

o	initial or trim value
1	in the 1st second
2	in the first two seconds
-80	inflight simulator terms (refers to 367-80 airplane)
LT	simulated "Large Transport" airplane terms
max	maximum
NB	nose boom
ss	steady state

SIMULATION SYSTEMS

Ground-Based Flight Simulator

The ground-based flight simulator used for these studies was the Ames Research Center moving-base transport simulator with a color television visual display. The visual scene, projected to simulate daylight flying, was produced by the Ames Research Center landing-approach color-image generator. The simulation solved the six-degrees-of-freedom equations of motion of the airplane and presented the solutions in cab motions, instrument readings, and visual display changes. Linearized aerodynamic coefficients were used in the equations of motion. The airplane ground effects were not included in the simulation.

The simulator utilized a transport-type cab with conventional seating, instrumentation, and controls for two pilots. The left hand seat was used for these tests. A hydraulic feel system was used to set control system force gradients. The general layout of the cockpit and instrument panel is shown in Fig. 1. The following instruments were provided:

Airspeed indicator
Altimeter
Rate of climb indicator
Angle of attack indicator
Angle of sideslip indicator
Turn and slip indicator
Compass
Attitude display
Localizer and glide slope error indicators (ILS)

Motion of the cab was controlled by three linear hydraulic servo actuators. These were operated differentially or synchronously for three degrees of freedom: roll, pitch, and heave (vertical). The roll axis of motion was scaled down so that a simulated roll angle of 10 degrees produced 5 degrees of cab roll motion. This reduced the side force due to bank angle that appeared to the simulator pilot as a spurious side force in a steady coordinated turn. Correct roll angles were displayed on the instruments and visual scene. A tabulation of the moving-base transport simulator physical characteristics is given in Appendix A.

The visual scene was produced by a closed-circuit color television system which utilized a scale landscape model including roads, buildings, and fields, as well as the runway to which the approaches were conducted. A color television camera was positioned by electric servos controlled by the simulation computer. The landscape model, camera, and mount system are shown in Fig. 2. The landscape model covered an area 2.5 miles wide and 9 miles long. Descent through a cloud layer was simulated by obliterating the picture above a preselected altitude. The tabulated physical characteristics of the visual display system are given in Appendix A. The pilot's outside view was limited to the visual TV scene by blocking out appropriate windows. Figure 3 presents an overall view of the cab including the TV screen and the TV projector.

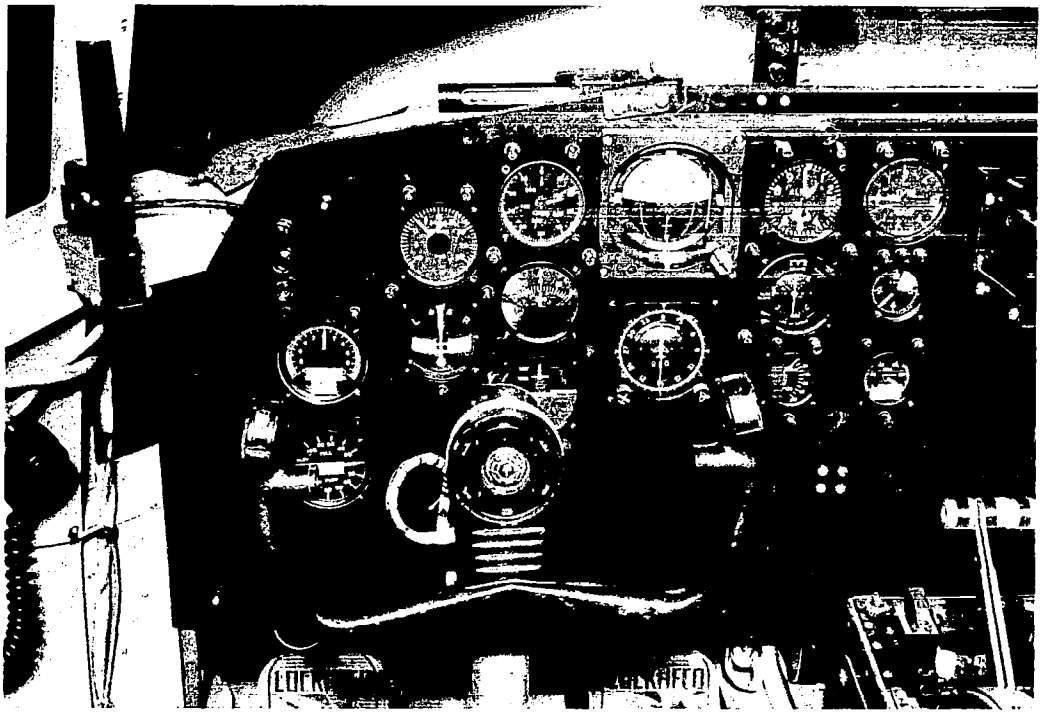

Figure 1. – NASA-Ames Moving Base Simulator Flight Deck

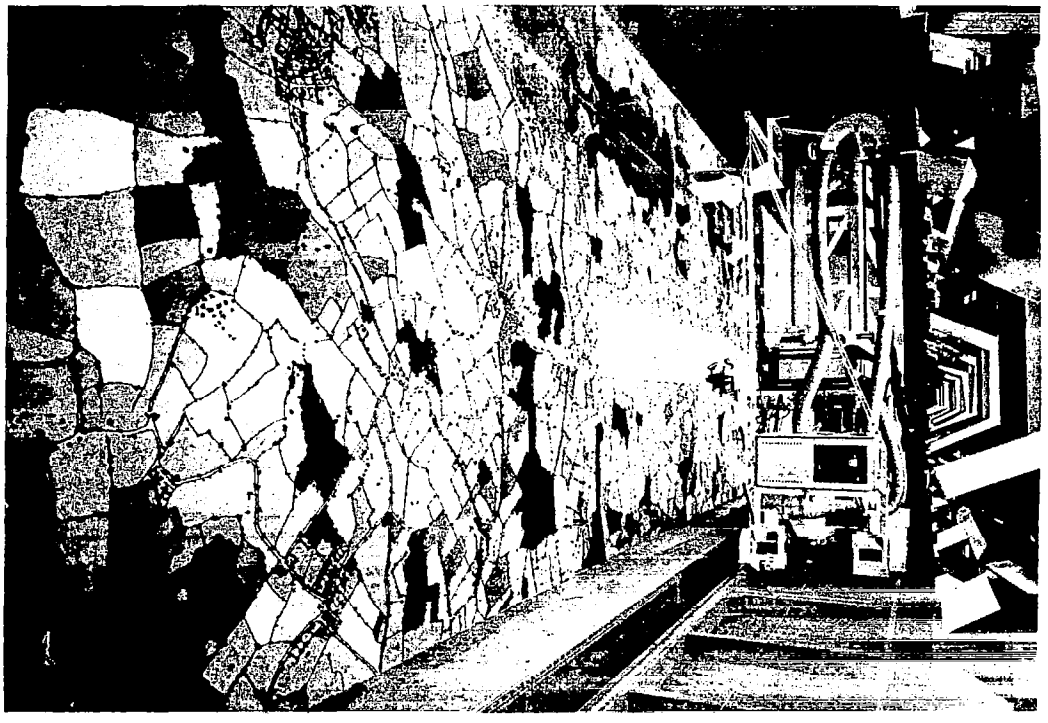

Figure 2. – TV Camera System with Model Runway and Landscape

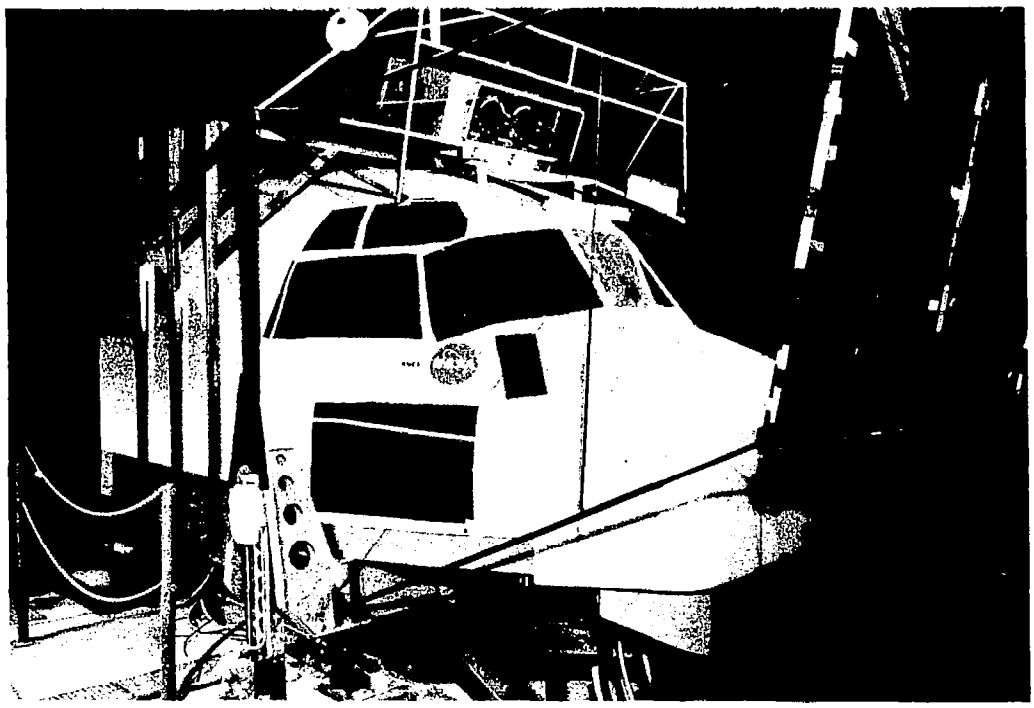

Figure 3. – NASA-Ames Moving Base Transport Simulator

Inflight Simulator

The inflight simulation system is conveniently divided into three subsystems for discussion purposes: the basic 367-80 airplane, the flight deck controls, and instrumentation and simulation equipment.

Basic 367-80 Airplane. — The airplane used for the inflight phase of the simulation program was the Boeing Model 367-80, shown in Fig. 4. A more detailed description of this airplane will be found in Appendix B. The 367-80 airplane was equipped as a variable stability airplane to simulate transport category aircraft. In the simulation configuration, five of the six degrees of freedom were controlled; lateral acceleration was not modified. An additional discussion of the variable stability capability of the 367-80 may be found in Ref. 1.

Flight Deck. — The flight deck of the 367-80 equipped for simulation is shown in Fig. 5. The left-hand seat was occupied by the safety pilot. The right-hand or evaluation pilot's station was equipped with a cockpit instrument system similar to that on present generation transports. The following basic display was provided:

Figure 4. – Boeing Model 367-80 Inflight Simulator

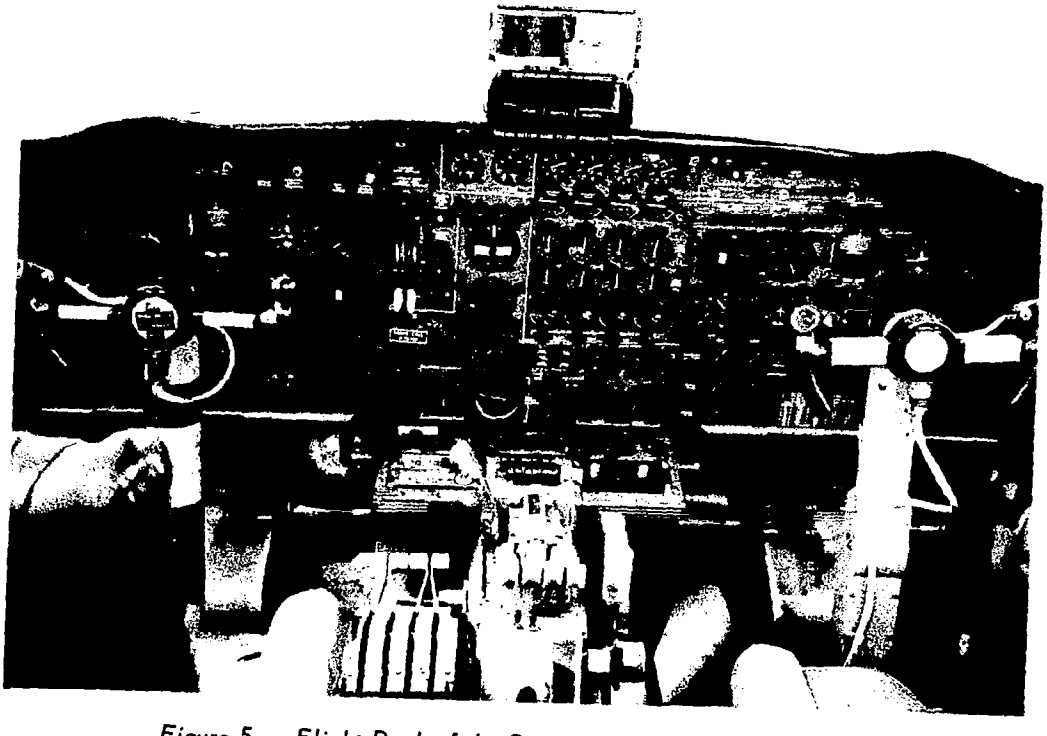

Figure 5. – Flight Deck of the Boeing 367-80 Inflight Simulator

Airspeed indicator
Altimeters (barometric and radar)
Instantaneous rate of climb indicator
Angle of attack indicator
Angle of sideslip indicator
Compasses (gyro, radio, ADF, and VOR)
Collins FD-108 flight director and integrated instrument system
Normal acceleration indicator
Control deflection and force indicators
Simulation limit lights.

The flight director displayed bank and pitch attitudes, and gave command information for VOR/ILS capture and tracking, altitude hold, and heading hold. Basic ILS error data were also displayed. The pilots used the flight director for most of the approaches flown during the program.

The evaluation pilot's control motions were converted to electrical signals by position transducers. The longitudinal column feel was produced by a mechanical detent to provide a breakout force and by an adjustable linear hydraulic spring. The lateral wheel force was produced by a fixed linear mechanical spring and a centering detent. Thrust control was by means of a single lever on the evaluation pilot's left side. Rudder control was by means of the basic 367-80 control system with the simulation signals superimposed upon the pilot input by means of a series servo.

The evaluation pilot had trim capability for all three axes. A switch on the pilot's wheel provided electrical series longitudinal trim, and a knob on the center pedestal provided electrical series lateral trim. Directional trim was through the normal 367-80 mechanical parallel trim on the center pedestal.

Simulation Equipment and Technique. — Computation for the simulation was performed on an 84-amplifier general purpose analog computer. The technique adopted for the simulation was essentially an open loop compensation technique in which the response of the airplane to a disturbance or command was modified by modulation of the airplane control surfaces. This response-feedback technique has the advantage of utilizing low loop gains in contrast to the analog model following system which must use high gain to achieve comparable performance. The rotational motions, pitch, roll, and yaw, were driven by the elevator, the lateral control (ailerons and spoilers), and the rudder, respectively. Lift was controlled by symmetrical motion of the spoilers, and drag by the engine thrust modulators. Control system dynamics were included in the analog computer. An example of the derivation of the control command equations is detailed in Appendix B.

Previous work indicated that because the 367-80 closely matched the geometry and flight speed of the simulated airplanes, the lack of aerodynamic side force control did not detract significantly from the simulation. No attempt was made to modify the basic 367-80 ground effect.

The following fundamental assumptions were made for the mechanization of the 367-80 as a variable stability airplane:

Linear aerodynamic derivatives and equations of motion (Function generators in the analog computer were adjusted to compensate known 367-80 nonlinearities.)
Constant gross weight and center of gravity
Instantaneous control surface response
Nonturbulent environment.

A more detailed discussion of the limitations of the inflight simulation may be found in Appendix B.

TEST PROCEDURES

The primary evaluation tasks for both ground and flight phases of this study were the approach and landing maneuver. The pilot performed an approach to the runway and continued through the flare to touchdown. The approach speed was 117 knots indicated air speed, the design value for the simulated airplane at 500,000 pounds.

For the lateral control studies, a lateral offset task (200-foot offset at 200-foot altitude) was selected as being the most demanding maneuver that the pilots were willing to perform close to the ground. Figure 6 presents an analysis of the side step maneuver using the methods of Ref. 2. As shown on the figure, a 200-foot offset correction initiated at 200-foot altitude requires approximately a 20-degree maximum bank angle and a 10-degree/sec maximum roll rate. Pilot comments from both Ref. 2 and this program indicated that a task which required more than a 20-degree bank angle would result in frequent landing aborts under service conditions.

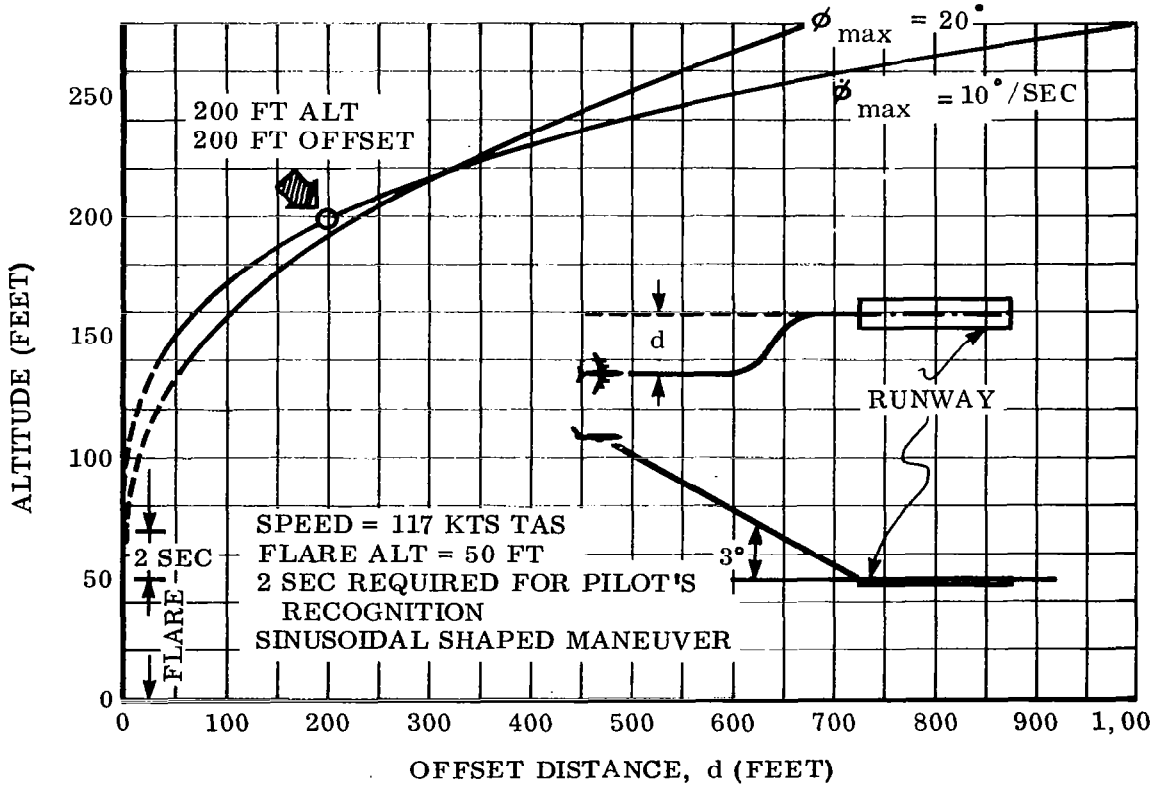

Figure 6. – Analysis of the Sinusoidal Sidestep Maneuver

Glide slope intercept from horizontal flight, glide slope tracking, and the landing flare were the significant longitudinal tasks.

Parameter variations around the basic configuration detailed in Appendix C were studied. The lateral parameters studied were control sensitivity, control power, rolling mode time constant, wheel force gradient, and the effect of control system response time. The longitudinal parameters studied were pitch control sensitivity, lift due to control, static stability, pitch damping, and lift curve slope. Column force gradient was not a variable. The ranges of the variables that were covered in the ground-based and flight simulations are shown in Table I. In order to evaluate only control requirements, the basic airplane was configured to meet the turn entry, aileron yaw, and yaw-due-to-roll-rate requirements for satisfactory STOL handling qualities indicated in Ref. 3.

Ground-Based Flight Simulator

The flight task used in the ground-based simulator was the landing approach and flare to touchdown. The pilots were allowed to fly as many approaches as they thought necessary to evaluate a configuration. After initial familiarization the pilots, in most cases, found one visual and one ILS approach adequate. The simulation was initiated approximately 6 miles from the runway threshold at an altitude of 1,000 feet and carried through to touchdown.

The ground-based simulation was checked for its validity prior to pilot evaluation using standard analog frequency and damping checks in conjunction with responses to control pulses which were compared against previously computed digital solutions. Documentation showing the measured characteristics of each configuration is presented in Appendix C.

In order to assess the effects of external disturbances on the roll control, some of the configurations were flown in simulated turbulence. The turbulence was introduced to the simulator as a rolling moment, angle of attack, and sideslip angle by filtering the output of a white noise generator through the following transfer function:

$$E_o/E_{in} = \frac{1}{0.59s+1}$$

The gains were adjusted to give a peak rolling acceleration of 0.15 rad/sec^2, with peaks of approximately 3 degrees in angle of attack and sideslip. This turbulence simulation was designed primarily to produce severe roll upsets with mild α and β excursions.

TABLE I

PARAMETER RANGES USED IN GROUND-BASED AND INFLIGHT SIMULATIONS

Parameter		Ground-based simulator		Inflight simulator		Units
		(Max)	(Min)	(Max)	(Min)	
Effective wheel angle	$\delta_{w_{eff}}$	90	30	50	30	deg
Control power	L_{max}	1.0	0.05	0.43	0.15	rad/sec^2
Rolling mode time constant	τ_R	1.59	0.6	1.14	0.36	sec
Control system response time	t_{max}	0.75	0	1.4	0.7	sec
Pitch control sensitivity	M_{δ_c}	+0.0646	+0.0141	+0.0625	+0.0167	$rad/sec^2/in.$
Lift due to control	L_{δ_c}	+0.004	-0.0059	-0.0001	-0.00635	rad/sec/in.
Lift curve slope	L_α	+0.925	+0.302	+0.645	+0.497	/sec
Static stability	M_α	-1.47	+0.245	-1.40	-0.13	$/sec^2$
Pitch damping	$M_{\dot{\theta}}$	-1.17	-0.242	-1.17	-0.59	/sec

Inflight Simulator

The maneuvers used in flight were divided into three main categories: configuration check, documentation of the configurations, and pilot evaluation maneuvers. Prior to any documentation or evaluation on a given flight, the configuration was checked using a standard pulse input to each control surface and a step input to the electrical throttle. The pulses were artificially generated in the computer. The airplane response was recorded and compared to the precalculated theoretical response of the simulated airplane (Fig. 7). The difference between test and theory indicates the combined effects of atmospheric turbulence and system uncertainties.

Having established total system response within acceptable tolerances by means of the configuration check maneuvers, several important characteristics were recorded in the documentation maneuvers. The lateral-directional documentation used the rate reversal technique of Ref. 3 to measure control power and sensitivity, isolated from other effects. The documentation maneuvers also included wheel steps from an initial bank angle to measure roll rate response and steady sideslips to measure static lateral-directional characteristics.

Longitudinal documentation used a pitch rate reversal maneuver similar to the lateral technique for measuring control power and sensitivity. A column step from steady level flight and a windup turn provided measurement of the pitch response and maneuvering characteristics. A moderate speed change from trim gave the static stability data. The documentation was completed by pilot excitation of the oscillatory modes of motion (short period, phugoid, and dutch roll) for measurement of period and damping.

The pilot evaluation maneuvers were the most important part of the program. They included both standardized control tests and actual landings. For evaluation of lateral control, the pilot performed heading changes of 5 degrees and 20 degrees, an S-turn, and a full wheel step. On lateral evaluation landings, a 200-foot lateral offset to the right of the runway centerline was programmed into the flight director. The pilot started the correction to the runway at an altitude of about 200 feet. Longitudinal pilot evaluation tasks consisted of a step column input, and pitch attitude changes of 5 degrees and 10 degrees in minimum time. One or two actual landings, including a simulated instrument approach, were performed with each configuration.

Four pilots participated in the ground-based evaluation while two evaluated the airborne simulation. All pilots were professional flight test pilots with recent experience in evaluation of handling qualities parameters for both inflight and ground-based simulations.

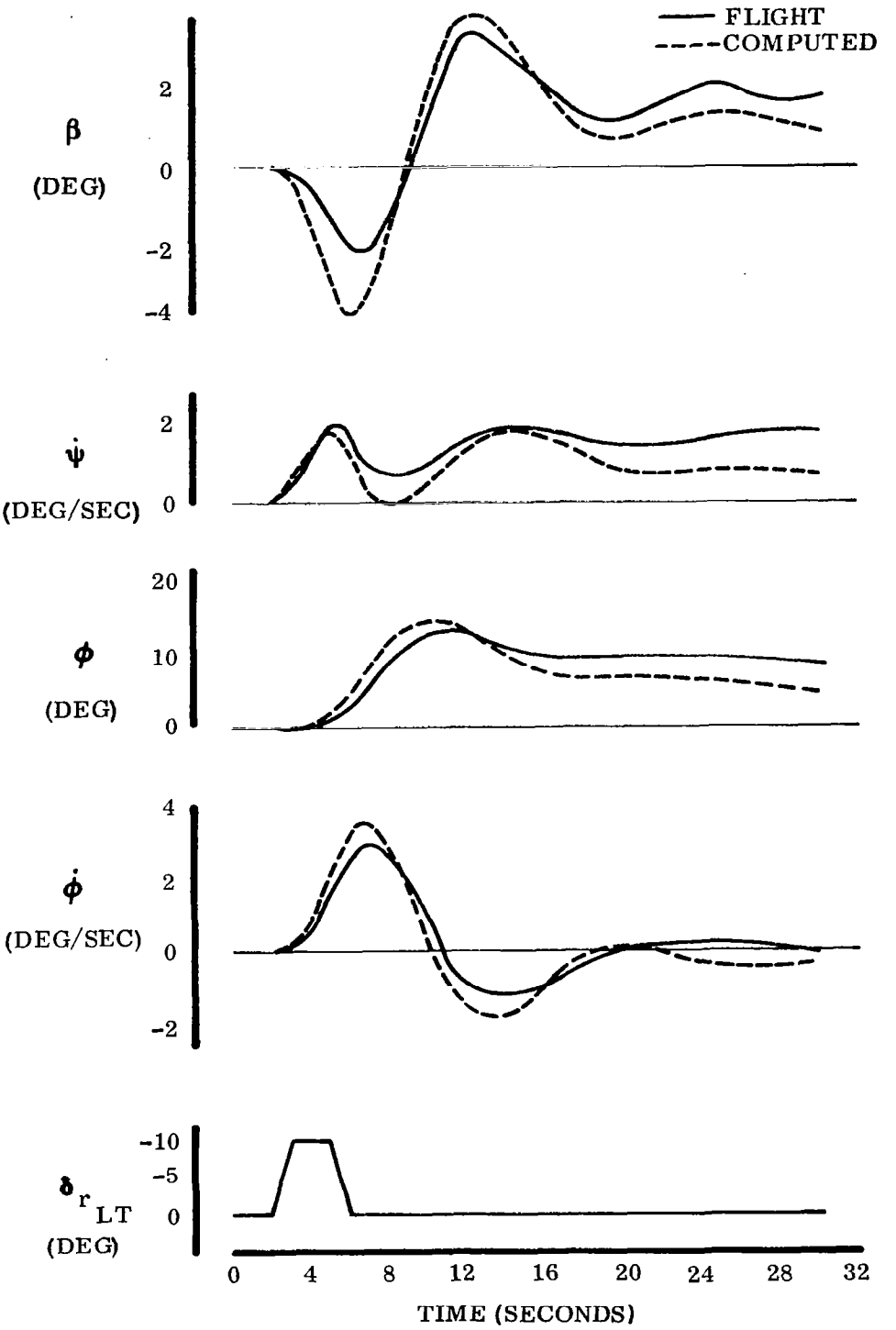

Figure 7. – Comparison of Flight and Computed Responses to a Rudder Pulse

RESULTS AND DISCUSSION

This investigation studied several problem areas for the large transport airplane in the landing approach. Although limited in scope, sufficient data were obtained to indicate significant trends for several important handling qualities criteria. The results are presented in the form of numerical pilot ratings of lateral control and longitudinal stability and control.

The pilots rated the handling qualities using the Cooper pilot rating system of Ref. 4 as summarized in Table II. Their opinions are presented as average ratings where more than one evaluation was available.

Lateral Control

The lateral control study was primarily concerned with the roll control sensitivity and roll power. The use of a nonlinear control system with capability to change both L_{max} and $\delta_{w_{eff}}$ allowed independent variation of sensitivity and control power, without changing the physical wheel stops as shown in Fig. 8. The wheel stops ($\delta_{w_{max}}$) were ± 90 degrees for the ground simulation and ± 75 degrees for the inflight simulation and were not changed during the test.

The effects of the rolling mode time constant, wheel forces, and control system response time were also evaluated.

Roll Control. — Maximum bank angle in the first second after initiation of wheel deflection ($\phi_{1_{max}}$) has been suggested as a figure of merit for roll control systems (Ref. 5). Quantitative use of this parameter requires specification of the method of calculation. The assumption of a single degree of freedom for airplane roll response allows a simple computation of roll acceleration, steady state roll rate, and roll time constant. However, as indicated in Fig. 9, when coupling with other degrees of freedom and substantial nonlinear characteristic exist, the roll response can be altered significantly. Accordingly, to avoid errors arising from the use of the single degree of freedom approximation, the values of $\phi_{1_{max}}$ used in this study were obtained from direct measurements of the actual airplane response with rudder pedals fixed.

The variation of pilot rating with $\phi_{1_{max}}$ for both ground-based and inflight evaluations is shown in Fig. 10. In the aggregate, the data show considerable scatter. Fifty per cent of the data are within ± 0.4 units of the mean and 90 per cent are within ± 0.9 units (Cooper scale). Lines of constant effective wheel angle ($\delta_{w_{eff}}$) faired through the data improve the correlation and suggest that the pilot is rating the bank angle response per wheel deflection or roll response sensitivity. If the data shown in Fig. 10 are presented in terms of the sensitivity parameter ϕ_1/δ_w (where $\delta_w \leq \delta_{w_{eff}}$), the four lines of constant wheel angle transform to the single line shown in Fig. 11. As plotted in Fig. 11, 50 per cent of the data are within ± 0.2 units and 90 per cent within ± 0.6 units of the mean. The significance of this parameter is indicated by the fact that a constant pilot rating of 3 was

TABLE II

PILOT OPINION RATING SYSTEM

	Adjective rating	Numerical rating	Description	Primary mission accomplished	Can be landed
Normal operation	Satisfactory	1	Excellent, includes optimum	Yes	Yes
		2	Good, pleasant to fly	Yes	Yes
		3	Satisfactory, but with some mildly unpleasant characteristics	Yes	Yes
Emergency operation	Unsatisfactory	4	Acceptable, but with unpleasant characteristics	Yes	Yes
		5	Unacceptable for normal operation	Doubtful	Yes
		6	Acceptable for emergency condition only*	Doubtful	Yes
No operation	Unacceptable	7	Unacceptable even for emergency condition*	No	Doubtful
		8	Unacceptable — dangerous	No	No
		9	Unacceptable — uncontrollable	No	No

*Failure of a stability augmenter

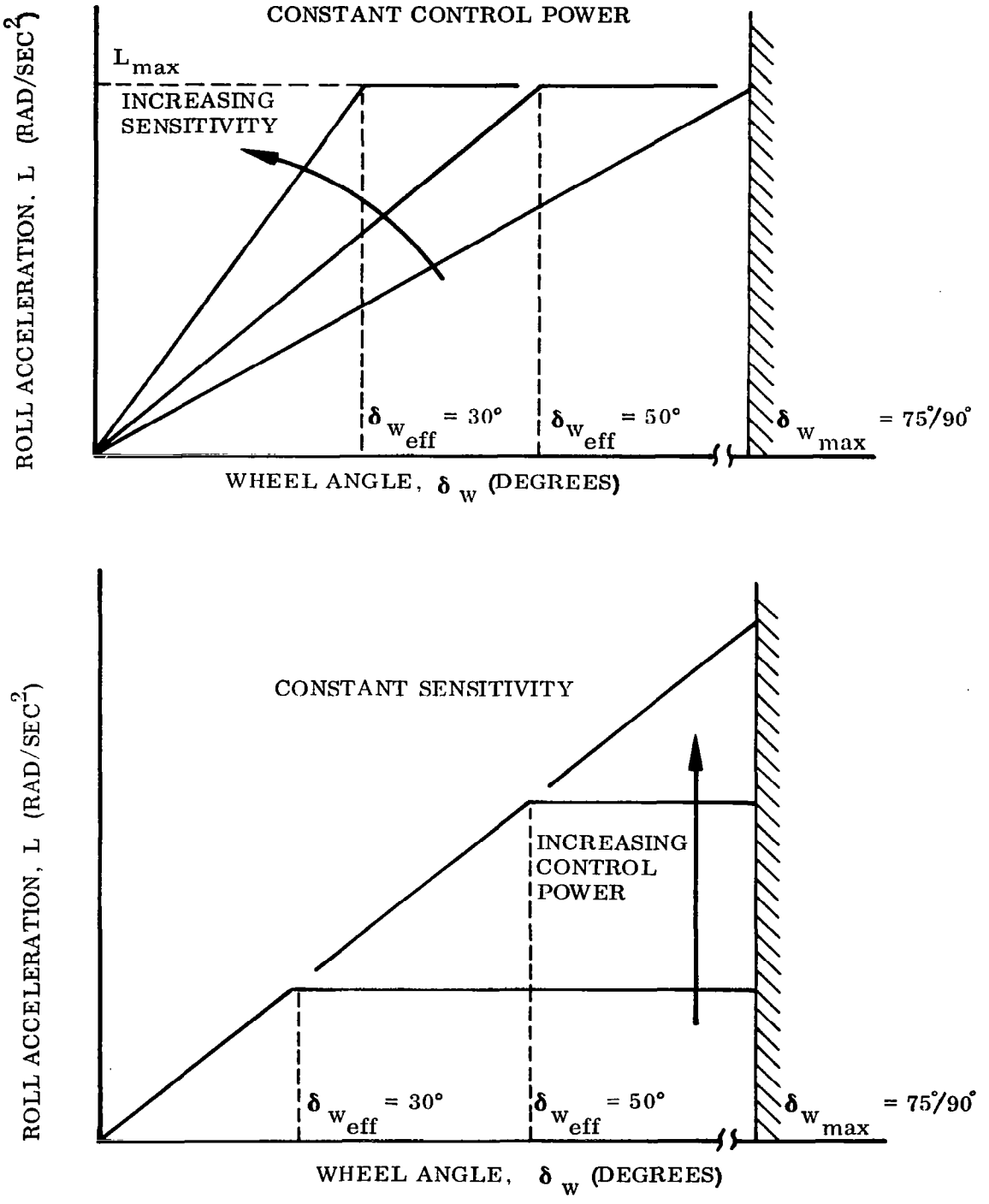

Figure 8. – Variation of the Roll Acceleration with Wheel Angle for Nonlinear Lateral Control System

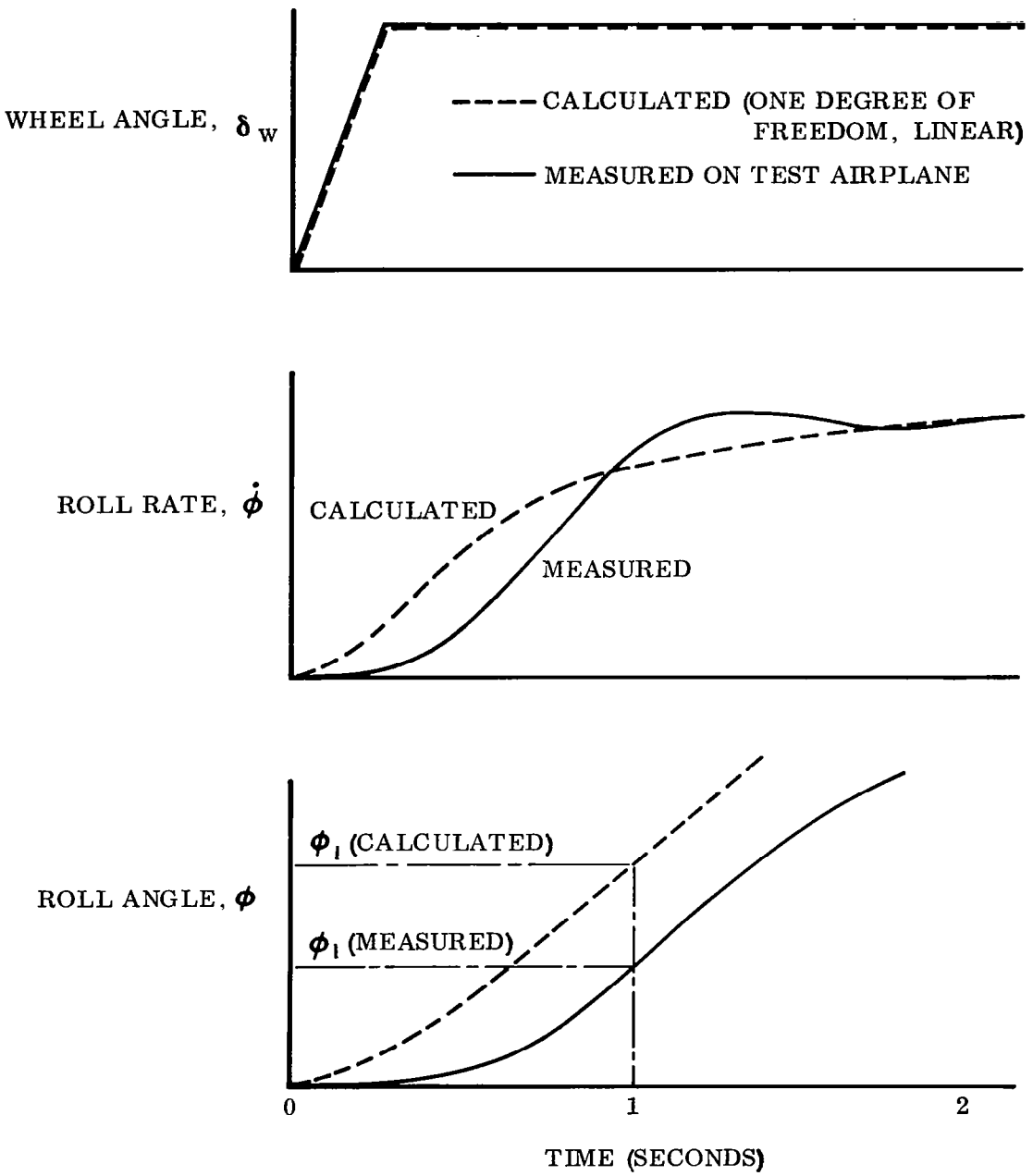

Figure 9. – Response to a Lateral Control Input for Fixed Rudder Pedal

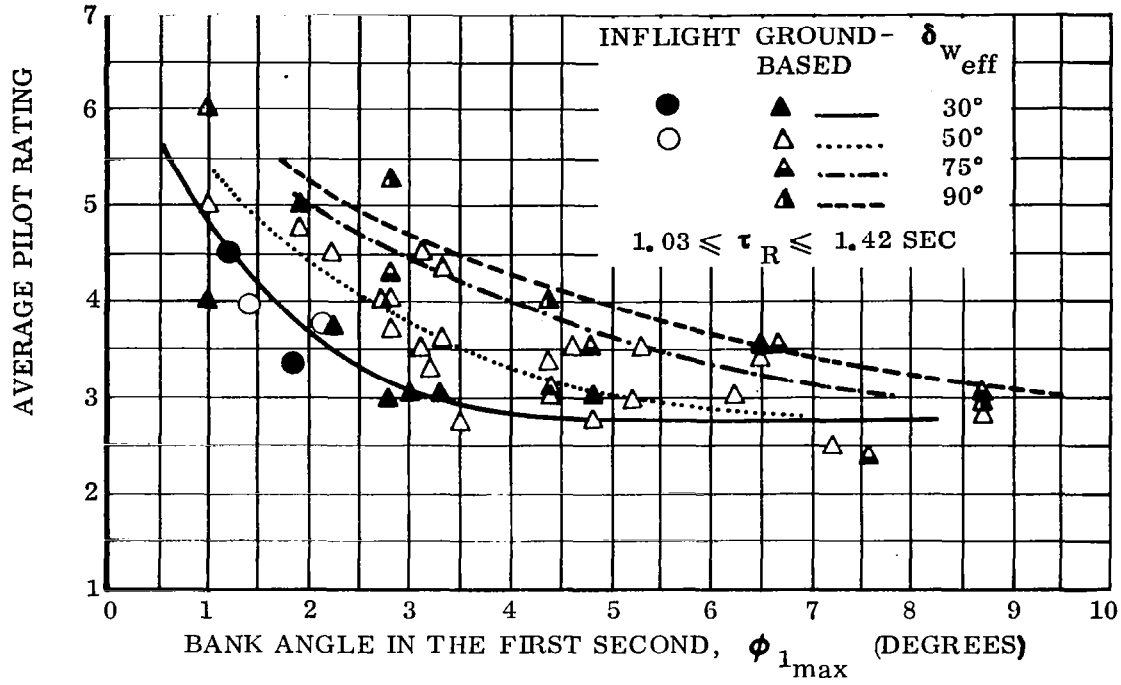

Figure 10. – Variation of Pilot Rating with Bank Angle in the First Second for Four Values of Effective Wheel Angle

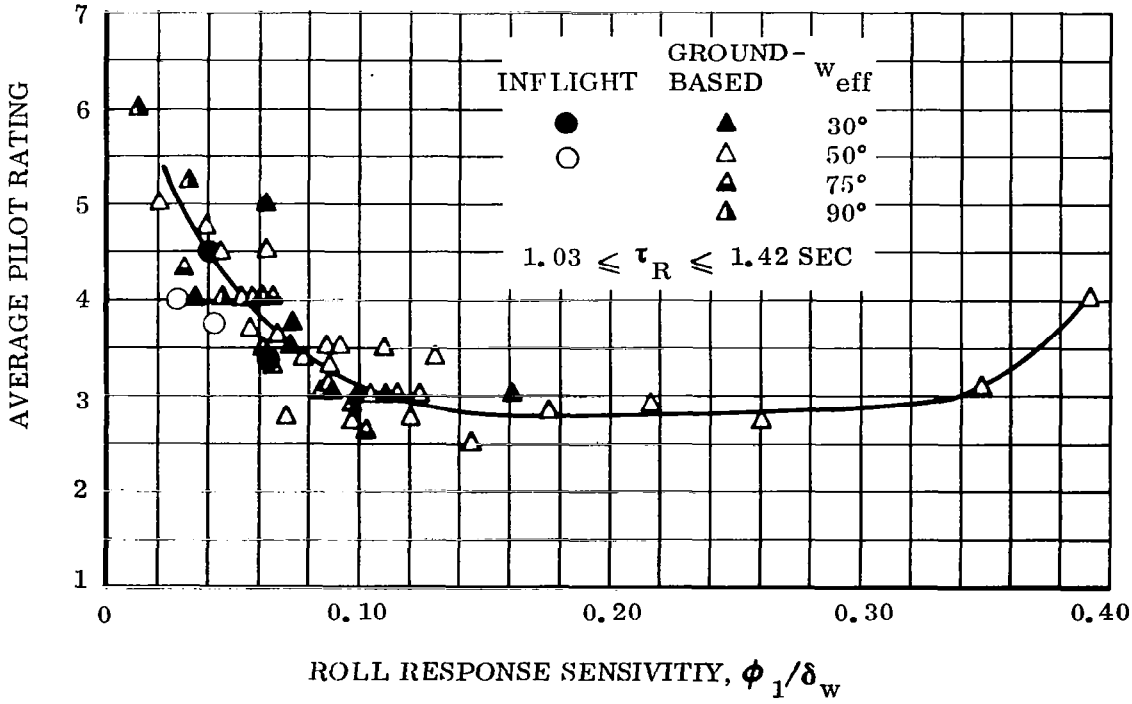

Figure 11. – Variation of Pilot Rating with Roll Response Sensitivity

obtained at a constant value of $\phi_1/\delta_w = 0.1$, while ϕ_{1max} varied from 3 degrees (δ_{weff} = 30 degrees) to 9 degrees (δ_{weff} = 90 degrees). The data were also plotted with ϕ_{2max} as a parameter; however, no improvement in correlation was obtained. These data are included in Tables III and IV of Appendix C.

An adequate evaluation of the nonlinear control system characteristics must include a task for which the pilot demands full lateral control. Figure 12 shows a typical time history of pilot's wheel motions for the 200-foot sidestep maneuver just prior to touchdown. Most of the lateral commands on the ILS approach were well within the linear range; however, the severity of required offset maneuver gave the pilot the opportunity to evaluate the nonlinear wheel characteristics. As shown, the pilot used wheel angles from stop to stop, well beyond δ_{weff} for which there was no increased rolling moment. There were no adverse pilot comments on the wheel nonlinearity, either for the ground-based or inflight simulators.

Figure 13 indicates that the addition of turbulence to the ground-based evaluation task did make the expected shift in pilot rating. Pilot opinion was degraded about 0.5 units on the rating scale for satisfactory control sensitivity. For lower sensitivity there was a more rapid degradation of pilot opinion than was found in smooth air.

Rolling Mode Time Constant. — The rolling mode time constant (τ_R) has been used as a handling qualities parameter. Computation of τ_R from the three-degree-of-freedom quartic characteristic equation provides a better approximation to the airplane roll response than that provided by the one-degree-of-freedom analysis. Accordingly, the values of τ_R presented in this report are the negative inverse of the rolling mode root of the characteristic equation. An increase in roll damping (which may be accomplished by means of stability augmentation) reduces the time constant.

Consistent with previous observations, pilot comments indicated that there was an improvement in handling qualities with increased roll damping. The improvement was seen as an ability to stop roll rate at a selected bank angle with less overshoot. This effect is indicated in Fig. 14 which is a time history of two 20-degree heading changes as documented in the inflight simulator. The upper two curves indicate a high level of wheel activity required to stabilize bank angle with a large roll time constant. The lower pair of curves show the reduction in oscillatory wheel motion accompanying a decrease in roll time constant. The precision of bank angle control was increased and the pilot rating improved from 3.4 to 2.9.

Figure 15 shows the improvement in pilot rating for decreasing values of roll time constant. The variation of roll response sensitivity (ϕ_1/δ_w) used in this evaluation was 0.092 to 0.32. As shown on Fig. 11, the pilot rating does not change for this range of sensitivities.

The effects of a short roll time constant on the pilot rating of roll response sensitivity (Fig. 16) indicate the same trends with regard to optimum sensitivity as for the longer time constant case. The overall improvement is about 1.0 on the Cooper scale.

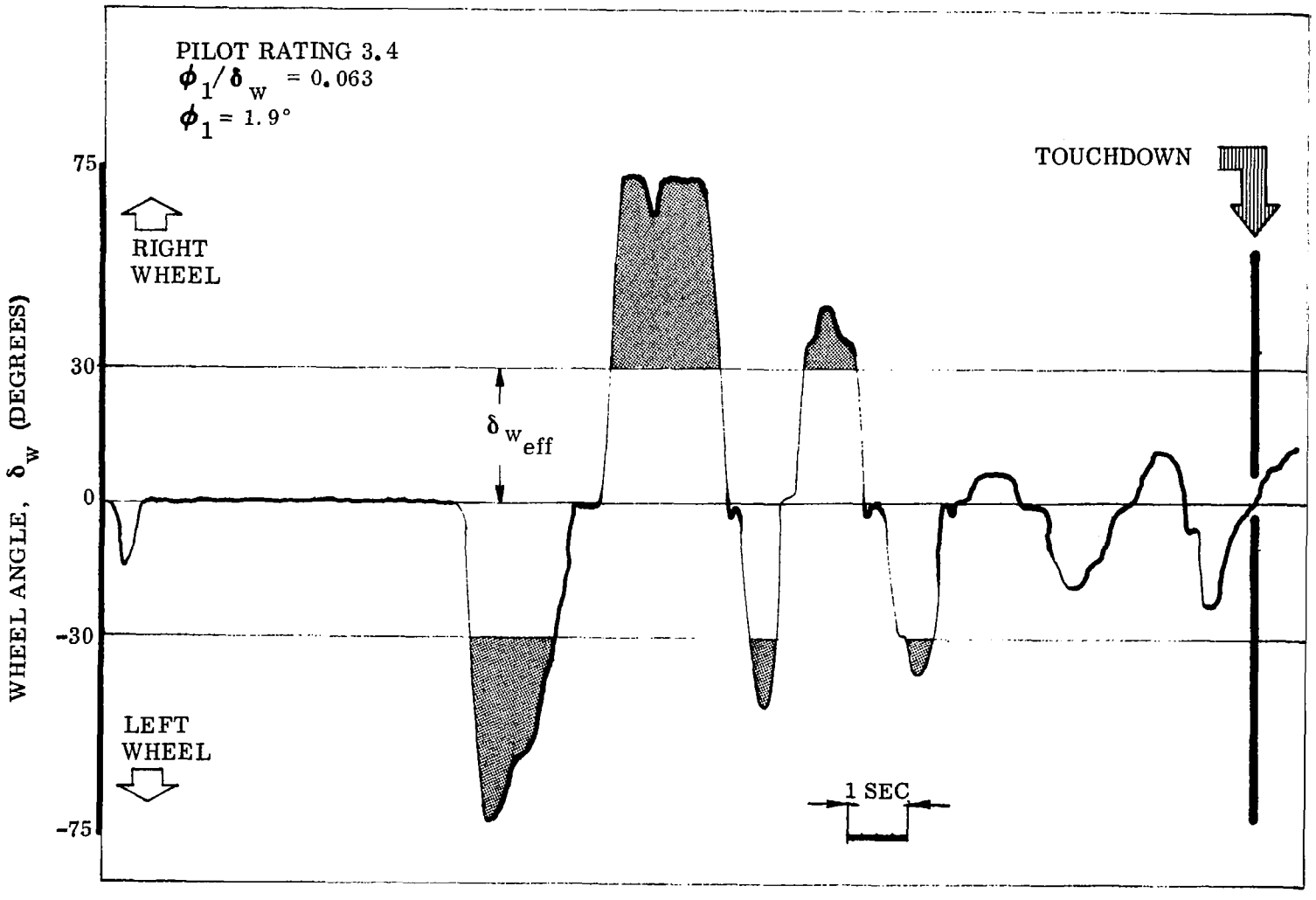

Figure 12. – Time History of Wheel Motion During Sidestep Maneuver

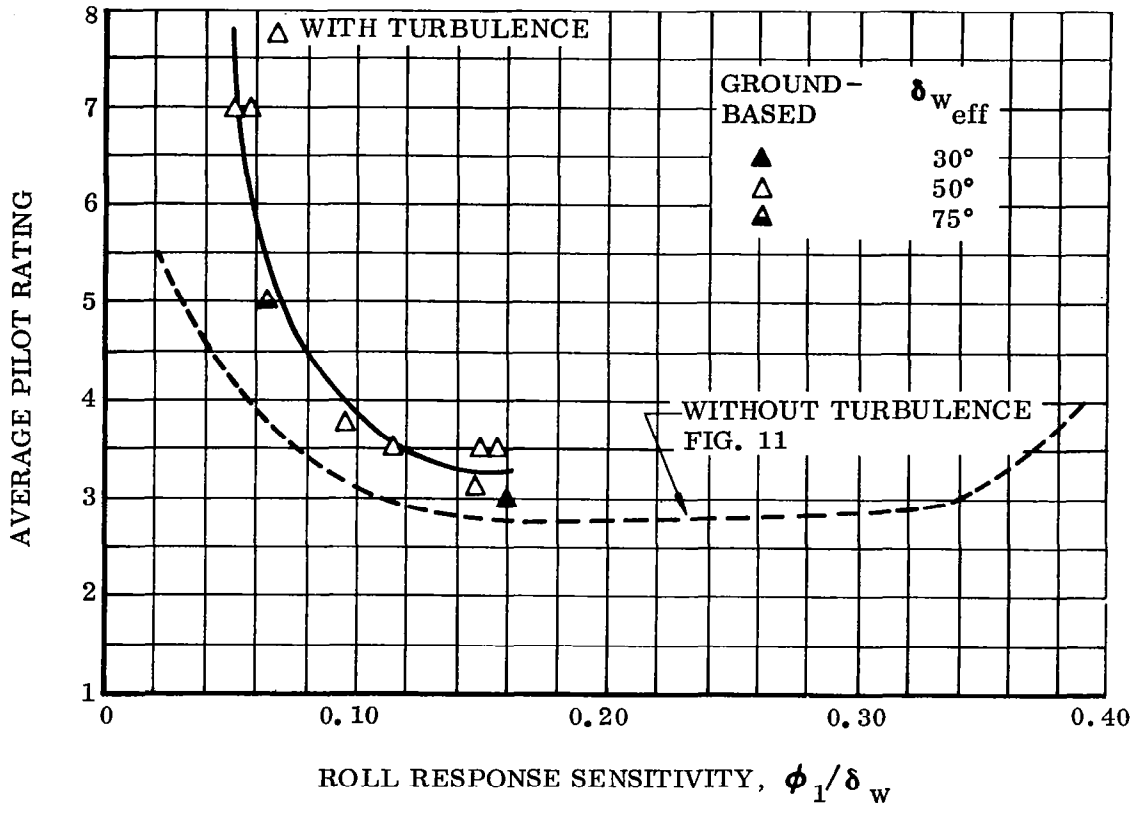

Figure 13. – Variation of Pilot Rating with Roll Response Sensitivity in Turbulence

Control System Characteristics. — The two control system characteristics considered in this study as being of primary concern to large airplanes were control system response time and control wheel forces.

The control system response time (t_{max}) is a composite measure of the control dynamics and approximates the effects of pure time lags, cable stretch, system rate limit, aerodynamic lags, and airplane flexibility. In order to study the effects of t_{max} on pilot opinion, t_{max} was varied by changing one component, the system rate limit. The rate limit was applied between the control wheel and the control surface and thus did not affect the wheel force characteristics.

The relationship of maximum roll acceleration, L_{max}, ϕ_{1max}, and t_{max} is shown in Fig. 17. These characteristics were computed for a roll time constant of 1.14 seconds. This figure was used to determine response time, t_{max}, for the flight conditions using measured values of ϕ_{1max} and L_{max}. As shown in Fig. 18, the pilot rating deteriorated for t_{max} greater than about 0.7 seconds. The pilots described this characteristic as being reflected in an apparent increased roll time constant for large wheel deflections.

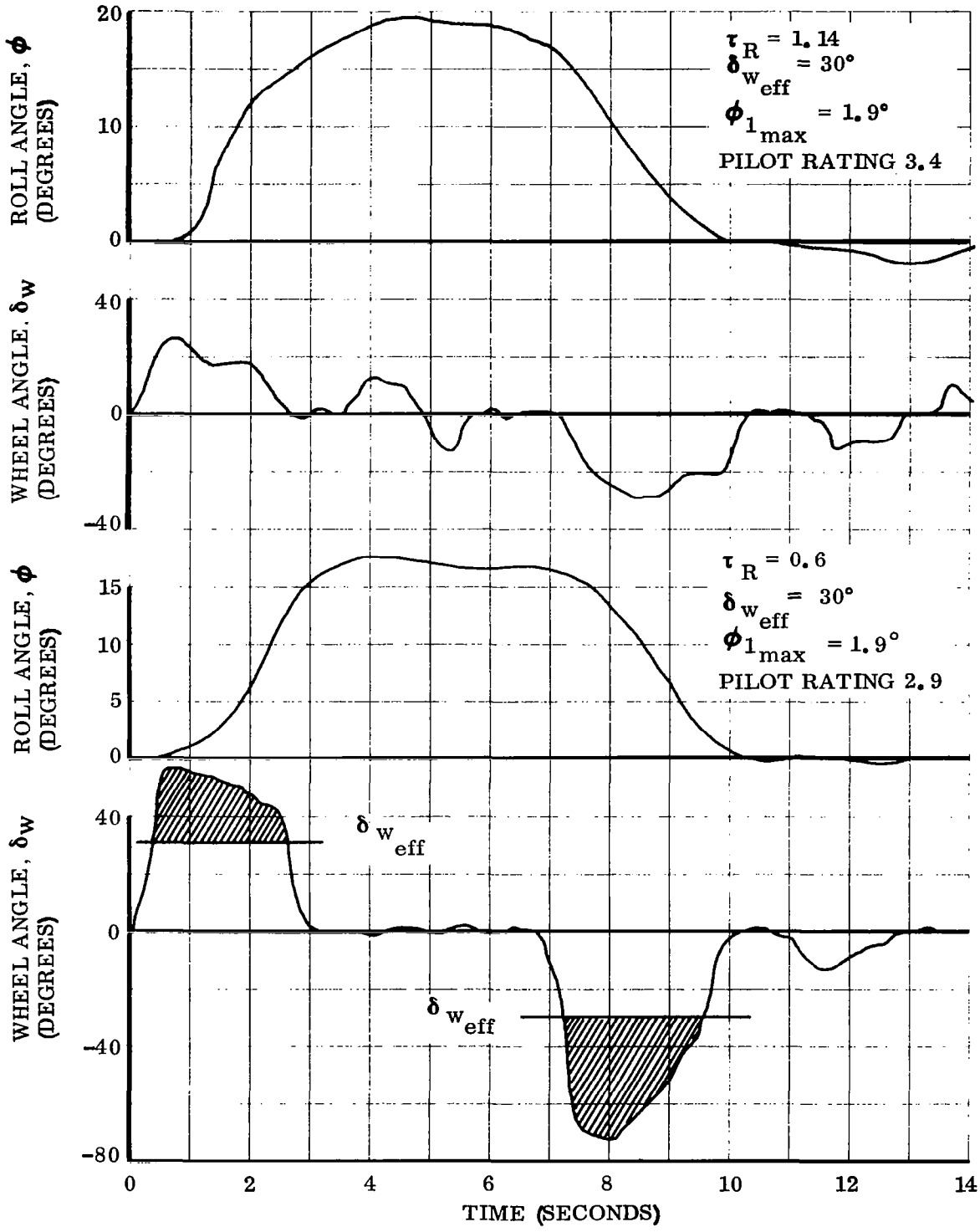

Figure 14. – Time History of 20-Degree Heading Changes Showing the Effect of Roll Time Constant on Wheel Motion

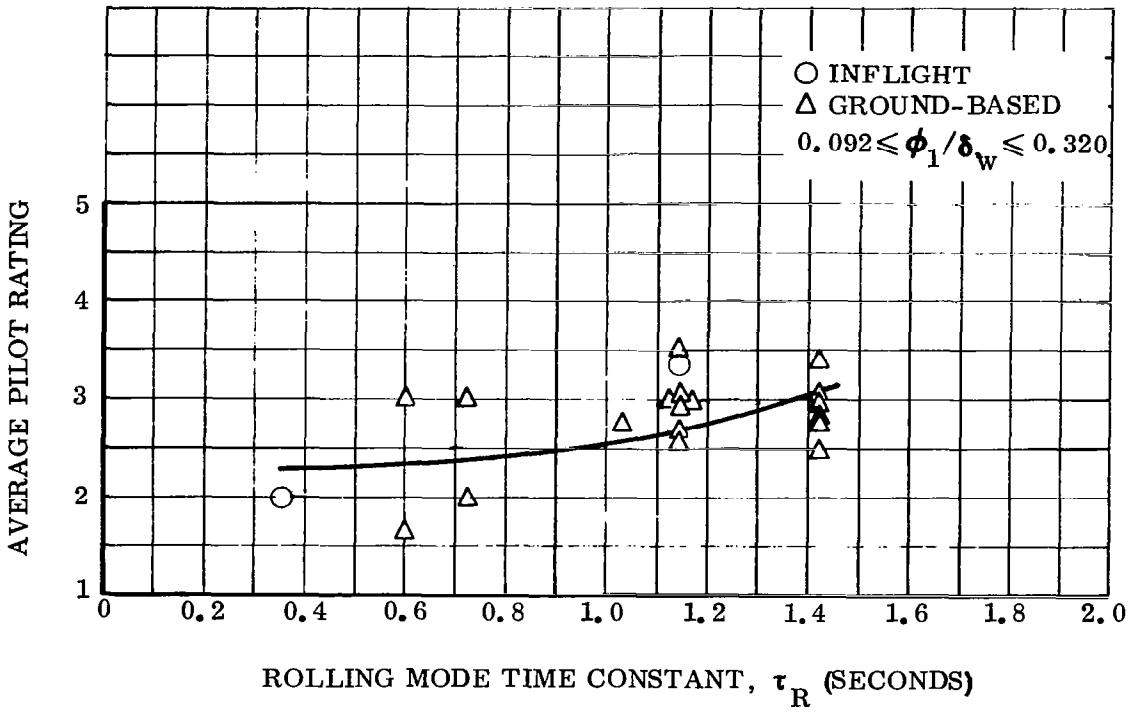

Figure 15. – Variation of Pilot Rating with Rolling Mode Time Constant

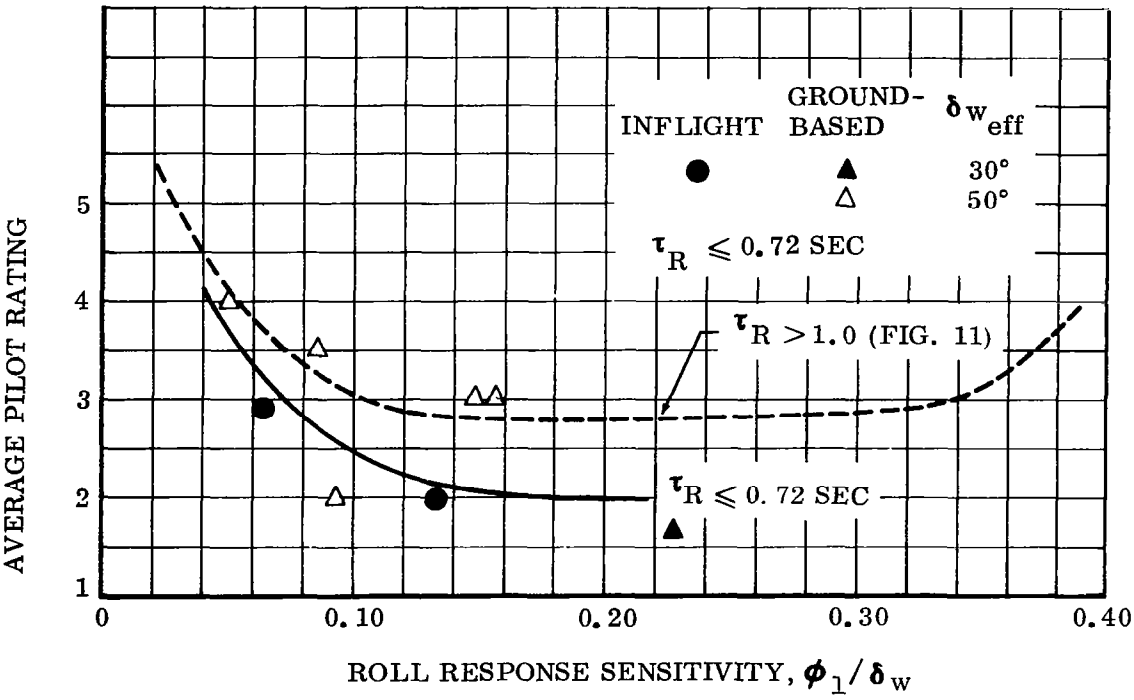

Figure 16. – Pilot Ratings of Roll Response Sensitivity Showing the Effect of Roll Time Constant

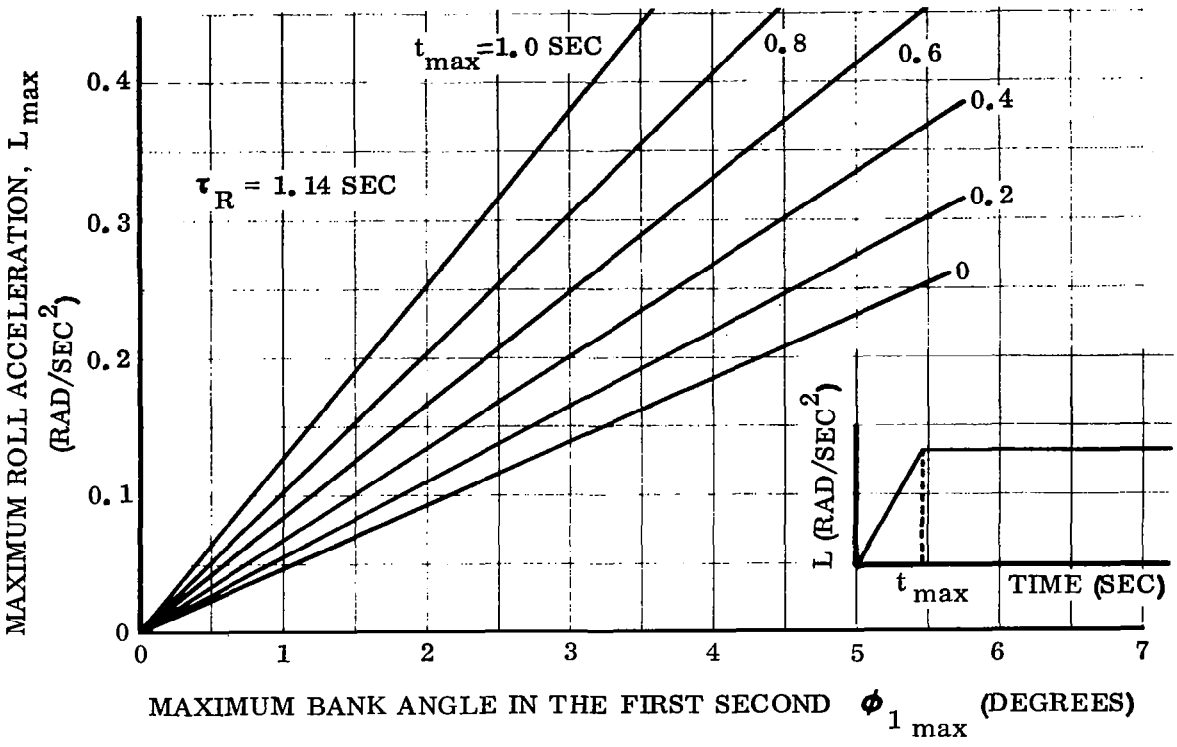

Figure 17. – Relationship of Roll Acceleration, Roll Response, and Control System Response Time

The effect of wheel force gradient on pilot opinion is presented in Fig. 19 as evaluated by one pilot. The lower limit of wheel force gradient was not defined in these tests. The pilot indicated that the lateral control forces would be dictated, to a large extent, by longitudinal control forces, and that the force gradient used in flight (0.2 lb/deg) and on the ground-based simulator (0.28 lb/deg) for most of the tests provided good force harmony between the wheel and column. The wheel breakout force was held constant for all tests at approximately 4 pounds to give positive centering.

Lateral Control Criteria. — Among the roll control criteria proposed in previous studies are maximum bank angle in the first second (ϕ_{1max}), maximum bank angle after two seconds (ϕ_{2max}), steady state roll rate (ϕ_{ss}), maximum roll acceleration (L_{max}), and roll time constant (τ_R). Over the range of values tested in this investigation, roll response sensitivity as measured by ϕ_1/δ_w correlated well with pilot opinion.

Figure 20 presents this criterion in terms of pilot rating boundaries showing an area for satisfactory sensitivity (pilot rating of 3 or better). The boundaries for minimum ϕ_{1max} and minimum δ_{weff} were not determined in these tests. This omission is not serious since, for practical aircraft, there are other requirements which demand certain values of lateral control power. As the requirements for ϕ_{1max} decrease, these other requirements establish the criterion for the lateral control power.

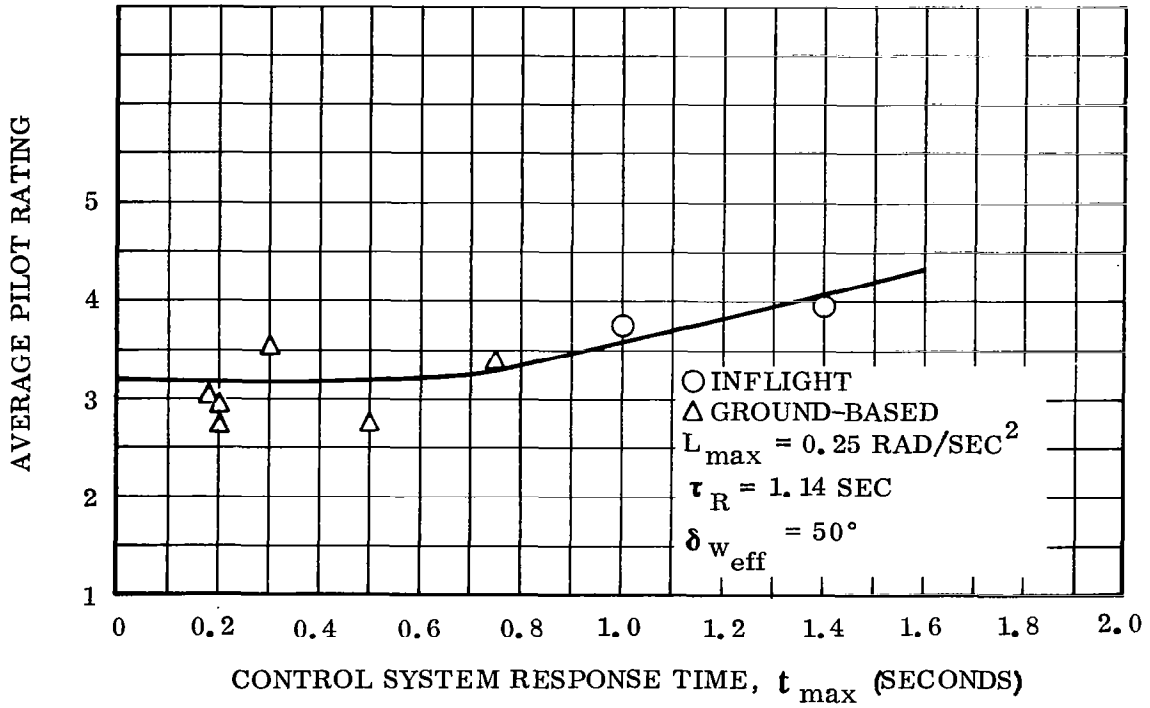

Figure 18. – Variation of Pilot Rating with Control System Response Time

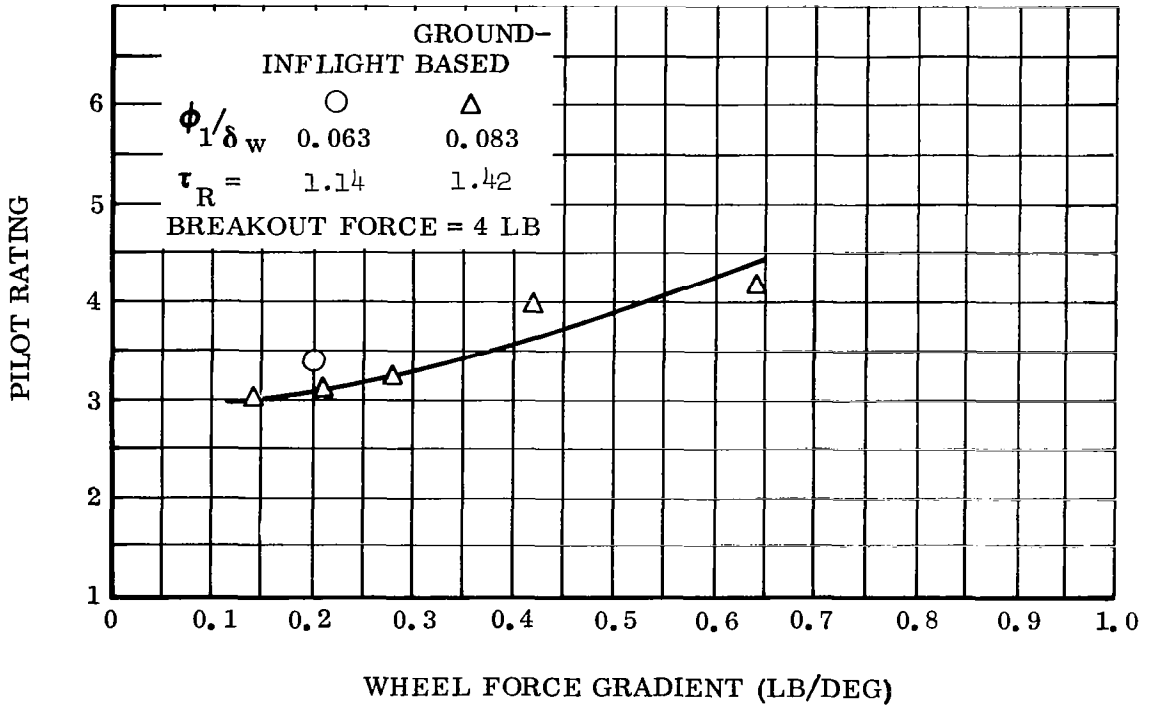

Figure 19. – Variation of Response Time with Wheel Force Gradient

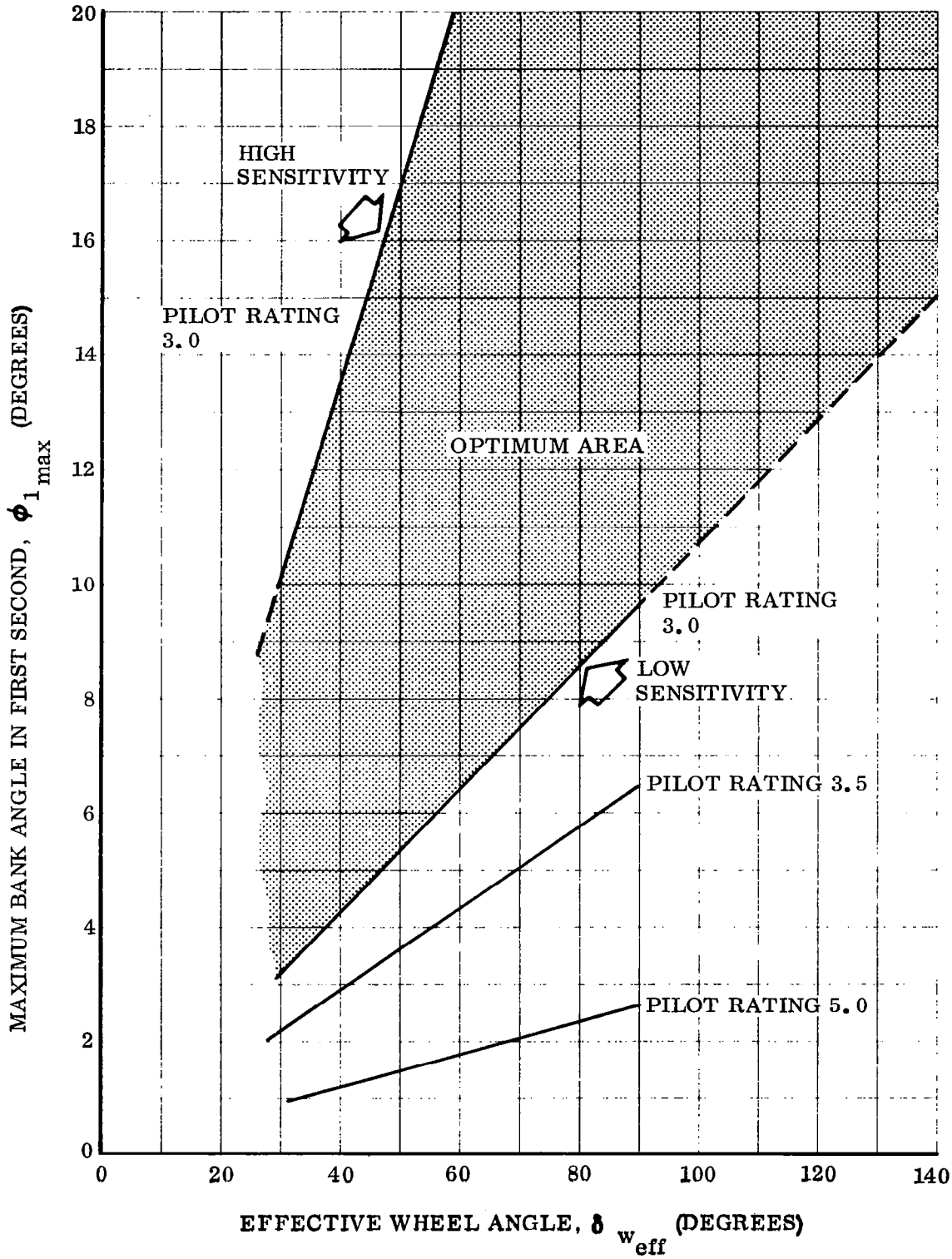

Figure 20. – Pilot Rating Boundaries for Roll Response Sensitivity

Longitudinal Stability and Control

In previous studies of large airplane handling qualities (for example, Ref. 6), pilots have commented adversely on "sluggish" response. The basis of this comment has not been fully understood. Accordingly, in an attempt to provide an understanding of the factors involved, variations in the following parameters were examined: pitch control sensitivity, lift due to control deflection, pitching moment due to angle of attack, pitching moment due to pitch rate, and lift due to angle of attack.

Control force gradient was not a variable in the program; however, pilots were given an opportunity to choose a level of control force they considered satisfactory. The column force gradient was selected as 6 lb/in. on the inflight simulator and set at 4.5 and 6 lb/in. on the ground-based simulator. Both simulators used a centering detent with a nominal 4-pound breakout force.

Longitudinal Control Sensitivity. — In the longitudinal evaluation, pilot opinion was strongly influenced by control column sensitivity as measured by pitch acceleration per unit control column deflection, M_{δ_c}. The variation in pilot rating with pitch control sensitivity is shown in Fig. 21 with several values of lift due to control deflection. There is a rapid deterioration in pilot opinion for M_{δ_c} below 0.03 rad/sec^2/in.

Lift Due to Control Deflection. — For airplanes with low values of short period frequency, it has been shown that flight path dynamic response is adversely affected by the lift loss associated with conventional aft control surfaces (Ref. 6). Figure 22 shows the lag in flight path response produced by lift due to control deflection, L_{δ_c}. Increasing the loss of lift due to control motion results in a degradation of pilot opinion as shown in Fig. 21. The differences in pilot rating due to L_{δ_c} are seen to be significant, particularly at low values of M_{δ_c}. The desirability of including this affect in defining a longitudinal control criteria is developed in a later section of this report.

Static Stability and Damping. — The effect of short period dynamics on pilot opinion has traditionally been presented on the frequency-damping plane. Figure 23 shows pilot rating in this manner; however, iso-opinion lines have not been drawn because of inconsistencies in the data. These inconsistencies stem largely from variations of the control parameters L_{δ_c} and M_{δ_c} that occurred in this series. The strong effect of these terms is shown in Fig. 21. While the range of pilot ratings affected by L_{δ_c} and M_{δ_c} was not large for the frequency damping variations, it does appear that the control parameters will modify pilot opinion.

A wide range of values of M_α was evaluated to assess the effect of static stability with approximately constant total damping, $\zeta \omega_n$. The data presented in Fig. 24 show that for constant M_{δ_c}, M_α has little effect on pilot opinion except for low or negative static margins. Increasing static stability improved the pilot rating except in the case of low control sensitivity. This latter trend may be explained by the high stick forces (a maximum of 194 lb/g) and reduced capability to maneuver for this case.

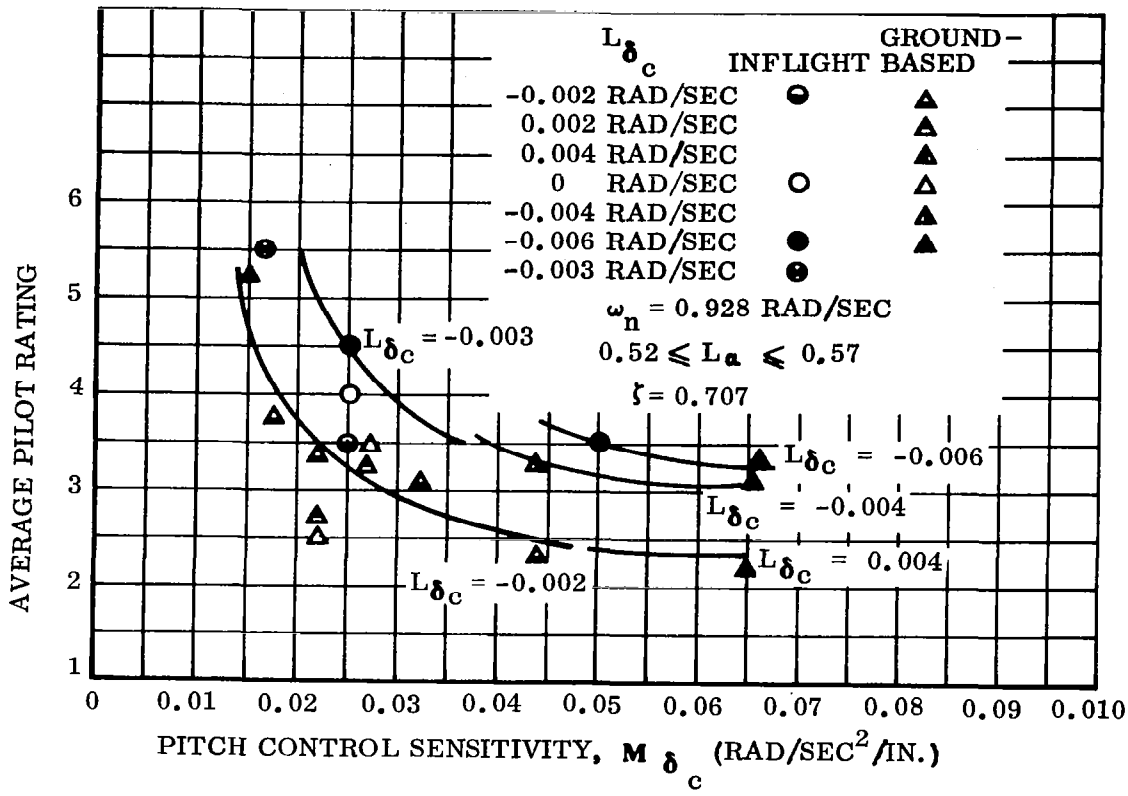

Figure 21. – Variations of Pilot Rating with Pitch Control Sensitivity and Lift Due to Control

For the base airplane, the pilot found it necessary to make a control reversal in order to prevent pitch overshoot when performing a change in pitch attitude. One explanation of this phenomena may be that the airplane has insufficient pitch rate damping, $M_{\dot{\theta}}$. To investigate this possibility, tests were run with various values of $M_{\dot{\theta}}$. The results are shown in Fig. 25. For the range tested, there was little effect of $M_{\dot{\theta}}$ on pilot opinion with M_{δ_c} and M_α constant. Based on pilot comments, the invariant rating was the result of two offsetting effects; the increased damping produced the desired reduction of pitch angle overshoot but also produced an undesirable increase in pitch stability or stick force per g.

Lift Curve Slope. — Large changes in lift curve slope, L_α, (0.3 to 0.9/sec) were made to determine the effect of lift curve slope on pilot opinion. The results of this parameter variation are shown in Fig. 26 for three values of static margins, M_α. A poor pilot rating is shown for high M_α and low L_α. This combination together with the low value of control sensitivity used in this part of the test made control over the airplane very difficult and produced a long period PIO tendency during the glide slope tracking task. Also associated with this combination was a high value (150 percent) of pitch rate overshoot which is defined as the ratio of maximum pitch rate to steady state pitch rate following a step command. For the short period frequencies typical of the unaugmented configuration of the simulated

airplane, large overshoot was not a problem. With the exception noted, it appears that lift curve slope had little effect on pilot opinion for the range of M_α tested.

Longitudinal Control Criteria. — The development of definitive criteria for longitudinal control characteristics was beyond the scope of this program; however, analysis of the data indicated that, as for the lateral case, the control sensitivity M_{δ_c} (as well as the related variable L_{δ_c}) was important to longitudinal handling qualities. Figure 27 presents the pilot rating data for various values of M_{δ_c} and L_{δ_c} for the basic frequency and damping. Although there were insufficient data to describe adequately the satisfactory boundary, the trends are apparent. Significantly, the curves indicate that as L_{δ_c} increases above a moderate level, increased M_{δ_c} will be necessary for adequate control. As noted, the boundary shown applies to the case represented by the basic airplane dynamics. For other stability characteristics the boundary may shift.

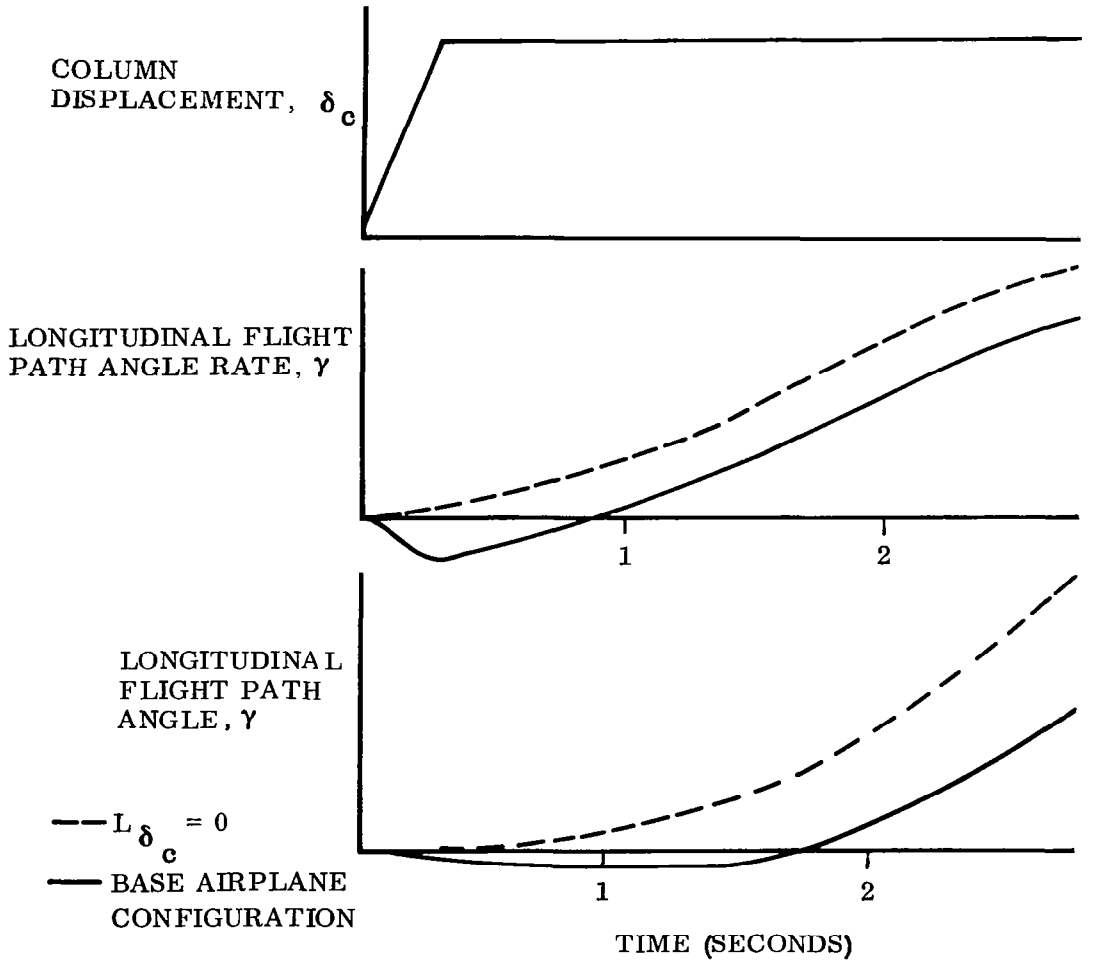

Figure 22. – Example of Flight Path Response to Elevator Input Showing the Effect of Lift Loss Due to Control Deflection

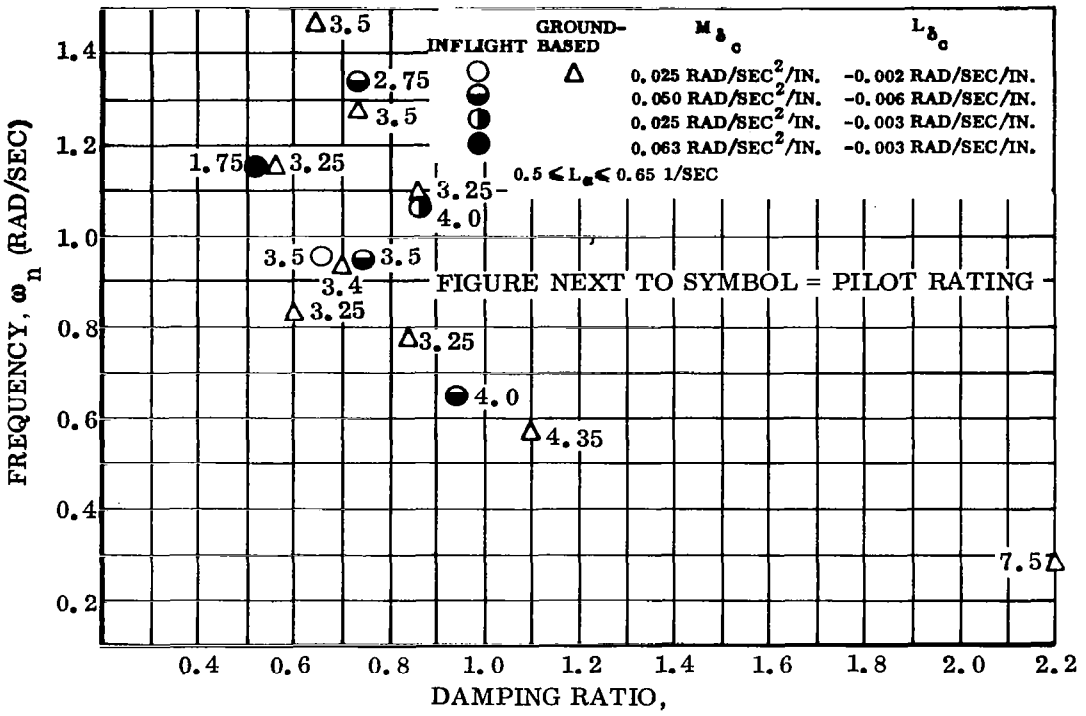

Figure 23. – Short Period Frequency and Damping Data

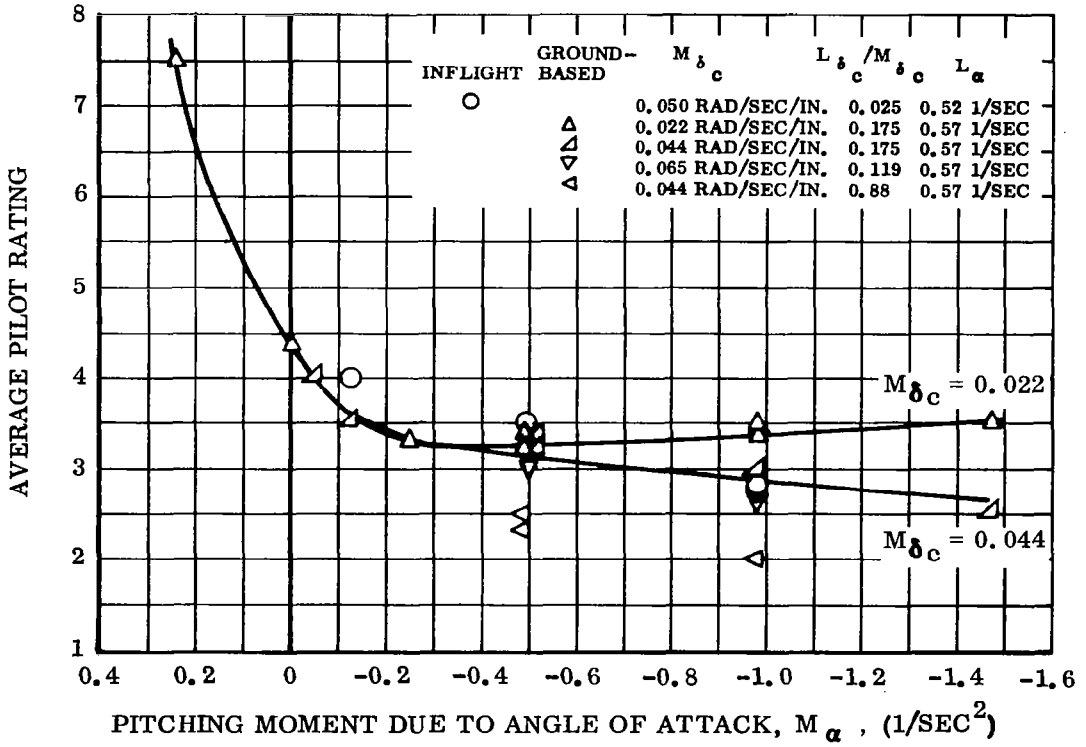

Figure 24. – Pilot Rating Variation with Static Stability Showing the Effect of the Control Sensitivity

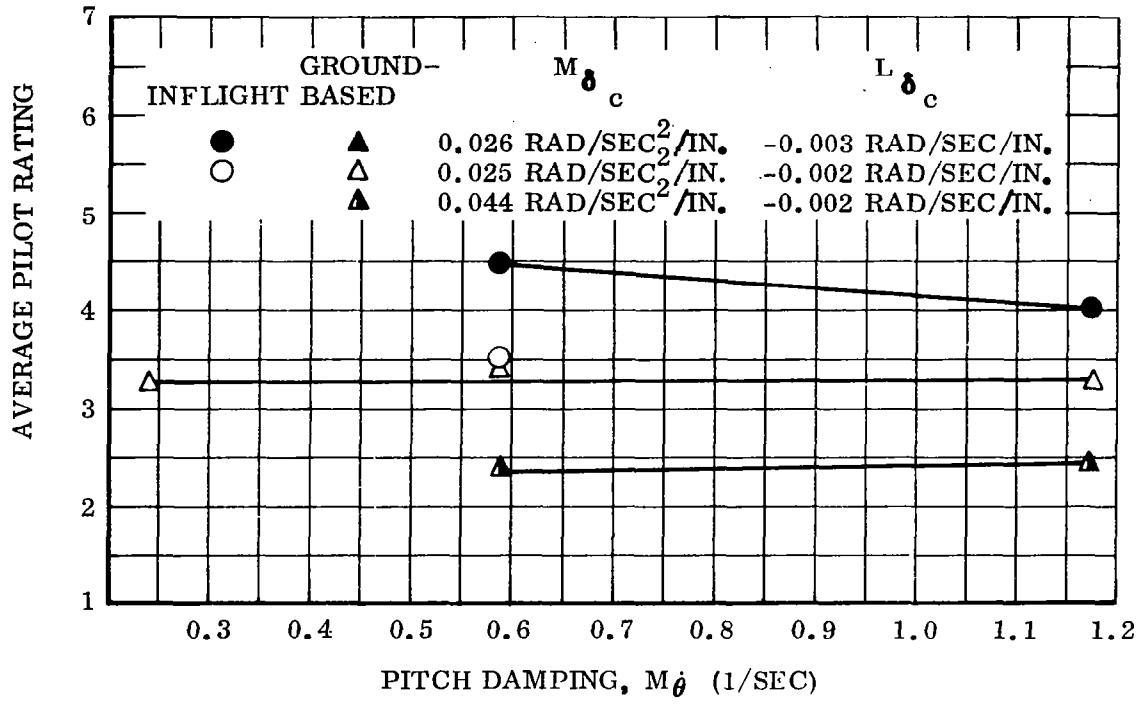

Figure 25. – Variation of Pilot Rating with Pitching Moment Due to Pitch Rate

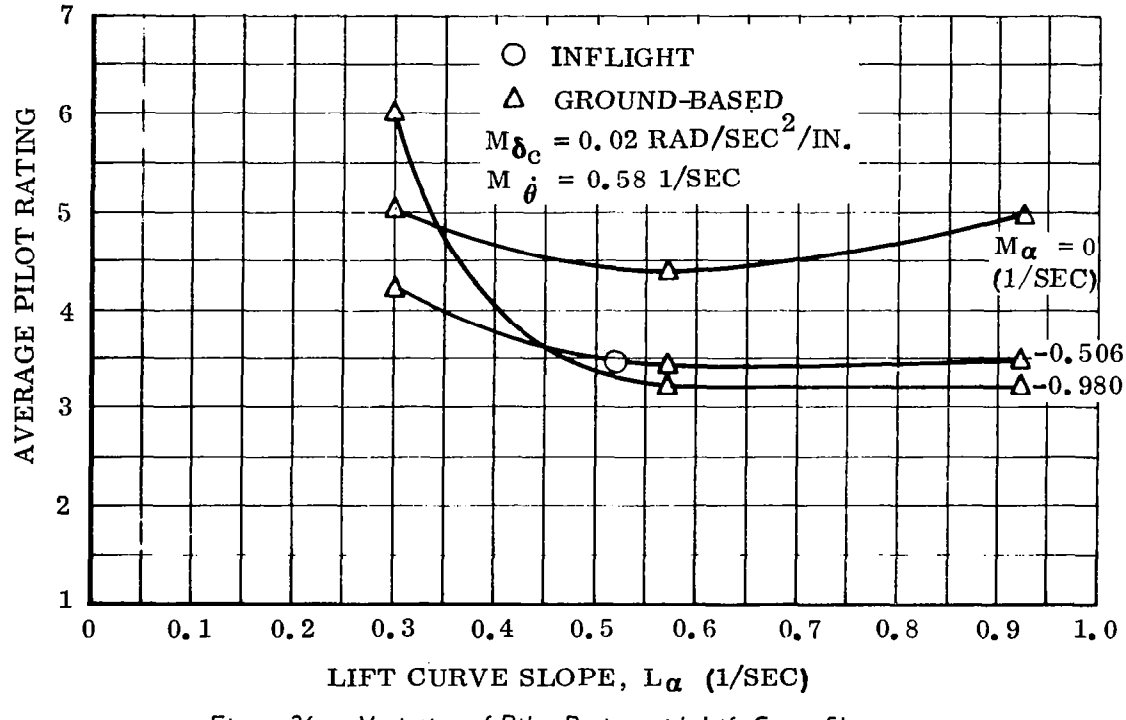

Figure 26. – Variation of Pilot Rating with Lift Curve Slope

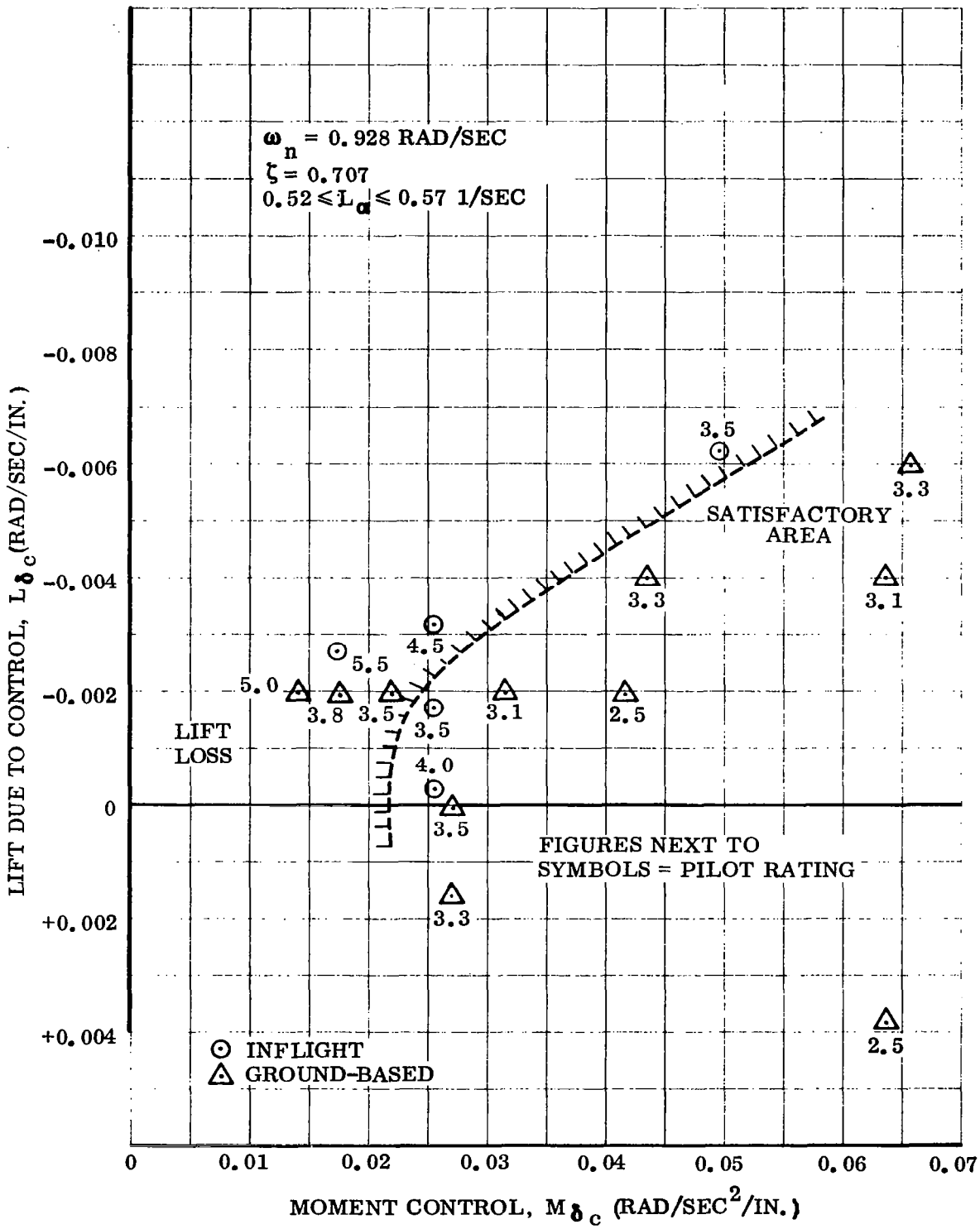

Figure 27. – Pilot Rating Boundary for Pitch Control Sensitivity and Lift Due to Control

CONCLUSIONS AND RECOMMENDATIONS

A coordinated ground-based and inflight piloted simulator program was conducted to study the problem areas associated with certain stability and control parameters of large transport class airplanes in the landing approach configuration. In particular, attention was directed to the factors that define required levels of lateral and longitudinal control.

Conclusions

This investigation has resulted in the following conclusions:

(1) Roll response sensitivity, as represented by ϕ_1/δ_w (bank angle attained in the first second per unit wheel), was found to be a correlating parameter for pilot rating for a range of effective wheel angles from 30 to 90 degrees.

(2) With a relatively low lateral control power, pilot opinion could be changed from unsatisfactory to satisfactory by a simple change in the control gearing (control sensitivity).

(3) As values of roll time constant increased from 0.35 to 1.4 seconds, there was a slight degradation of pilot opinion, but the pilot ratings were satisfactory for suitable control sensitivity.

(4) A boundary for satisfactory longitudinal control required consideration not only of control sensitivity (M_{δ_c}), but also of lift due to control deflection (L_{δ_c}).

Recommendations

To further clarify handling qualities criteria for large transport aircraft in the landing approach, the following investigations are recommended:

(1) An investigation of the relation of the wheel stops to the wheel angle for maximum rolling moment ($\delta_{w_{eff}}$) and their combined effect on pilot opinion should be conducted.

(2) The range of effective wheel angles below 30 degrees should be studied to define the minimum control power required for maneuvering large aircraft.

(3) A more complete definition of the effects of both L_{δ_c} and M_{δ_c} on pilot opinion is needed to establish longitudinal control criteria. Positive L_{δ_c} (canard or direct lift) should be studied as well as the negative values associated with conventional aft control airplanes.

(4) Configurations should be evaluated with longitudinal characteristics in the range of values obtainable with pitch axis augmentation.

APPENDIX A

GROUND-BASED SIMULATION SYSTEM CAPABILITIES

Tables A-I and A-II present the physical system capabilities of the Ames moving-base transport simulator and landing approach color television display.

TABLE A-I

Ames Moving-Base Transport Simulator

Motions Generated:	Maximum Acceleration *	Maximum Displacement *
Roll	1 rad/sec^2	±9 degrees
Pitch	0.5 rad/sec^2	+14 to -6 degrees
Heave (vertical)	±0.8 g (from ambient)	24 in.
* Assumes independent motion		

TABLE A-II

Ames Landing-Approach Color Television Display

Motions Generated:	Maximum Velocity	Maximum Displacement *
Roll	0.35 rad/sec	--
Pitch	0.52 rad/sec	--
Yaw	0.17 rad/sec	360 degrees
Lateral	240 knots	2-1/2 miles
Vertical	6000 ft/min	1,500 ft to 20 ft
Longitudinal	240 knots	9 miles
Runway length	--	10,000 ft
* Model scale 1:1200		

APPENDIX B

DESCRIPTION OF THE INFLIGHT SIMULATOR

The Boeing Model 367-80 is the prototype of the C/KC-135 jet transport/tanker airplanes and the 707 series commercial transports. The 367-80 has been used as a development test bed for improved flap systems, autopilot devices, and other airplane equipment. A two-view drawing and basic specifications are presented in Fig. B-1. As flown in this program, the 367-80 was equipped with fixed leading edge slats on the outboard section, Krueger flaps on the inboard section, and boundary layer control (BLC) trailing edge flaps. The BLC flaps are large chord with single pivot hinges. High pressure engine bleed air is blown over the upper surface of the flaps. The BLC system is shown in Fig. B-2 and discussed in detail in Ref. 7. This system was used during the program to simulate the high roll power and low roll time constant configuration. All other characteristics remained essentially unchanged from the base lateral configuration. The longitudinal BLC configuration was also documented.

Example of Control Command Derivation. Figure B-3 indicates the variables used in the computation of the control commands. The magnitudes of the electrical commands to the surfaces were obtained from precalculated differences between the response of the basic 367-80 airplane and the response of the simulated airplane. The calculations were based on the known stability and control derivatives of the 367-80 and the predicted derivatives of the simulated airplane.

Figure B-4 shows a simplified block diagram of the elevator system. The derivation of the elevator command equation illustrates the method used for each control surface. The first step is the requirement that all center of gravity accelerations, both linear and rotational, be identical for the 367-80 and the simulated airplane. Thus, for the pitch axis

$$\ddot{\theta}_{-80} = \ddot{\theta}_{LT}$$

Expanding this simple identity using a summation of pitching moments results in the following equation:

$$\left\{\frac{q_o\, S\bar{c}}{I_{yy}}\right\}_{-80} \begin{bmatrix} C_{M_{\delta_{th}}} & \delta_{th} \\ C_{M_{\alpha}} & \Delta\alpha \\ C_{M_{\dot{\alpha}}} & \dot{\alpha} \\ C_{M_{\dot{\theta}}} & \dot{\theta} \\ C_{M_{\Delta V}} & \Delta V \\ C_{M_{\delta e}} & \delta e \\ C_{M_{\delta_{ab}}} & \delta_{ab} \end{bmatrix}_{-80} = \left\{\frac{q_o\, S\bar{c}}{I_{yy}}\right\}_{LT} \begin{bmatrix} C_{M_{\delta_{th}}} & \delta_{th} \\ C_{M_{\alpha}} & \Delta\alpha \\ C_{M_{\dot{\alpha}}} & \dot{\alpha} \\ C_{M_{\dot{\theta}}} & \dot{\theta} \\ C_{M_{\Delta V}} & \Delta V \\ C_{M_{\delta_e}} & \delta_e \end{bmatrix}_{LT}$$

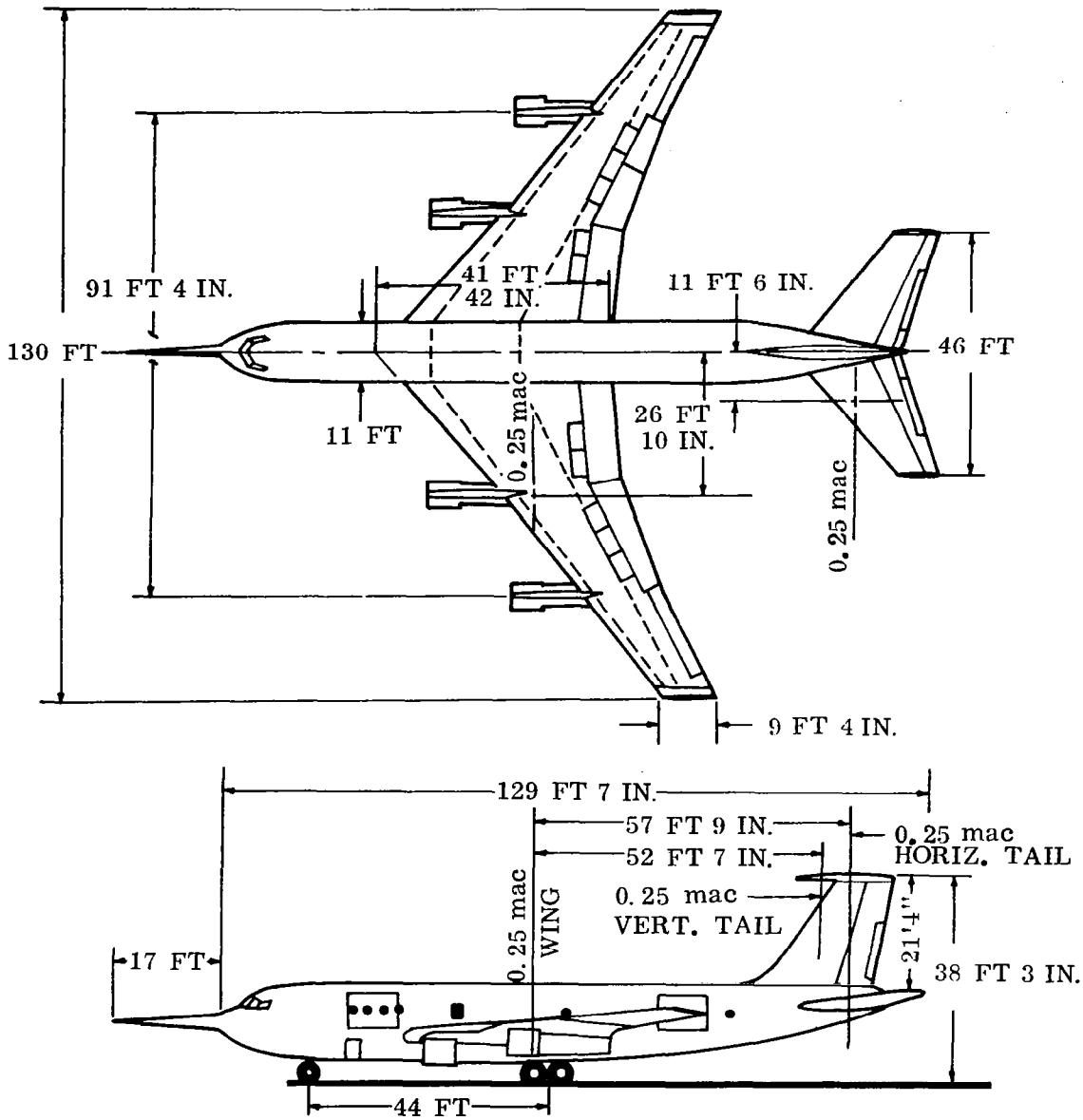

WING:			HORIZONTAL TAIL:			VERTICAL TAIL:		
AREA	2821.36	FT^2	AREA	625	FT^2	AREA	312	FT^2
ASPECT RATIO	6.0		ASPECT RATIO	3.37		ASPECT RATIO	1.46	
SWEEP (0.25c)	35	DEG	SWEEP (0.25c)	35	DEG	SWEEP	31.0	DEG
INCIDENCE	2.0	DEG	TAPER RATIO	0.421		TAPER RATIO	0.45	
DIHEDRAL	7.0	DEG	DIHEDRAL	7.0	DEG	TAIL VOLUME	0.0447	
MAC	20.05	FT	TAIL VOLUME	0.638				

Figure B-1. – Boeing 367-80 Inflight Simulator Geometric Data

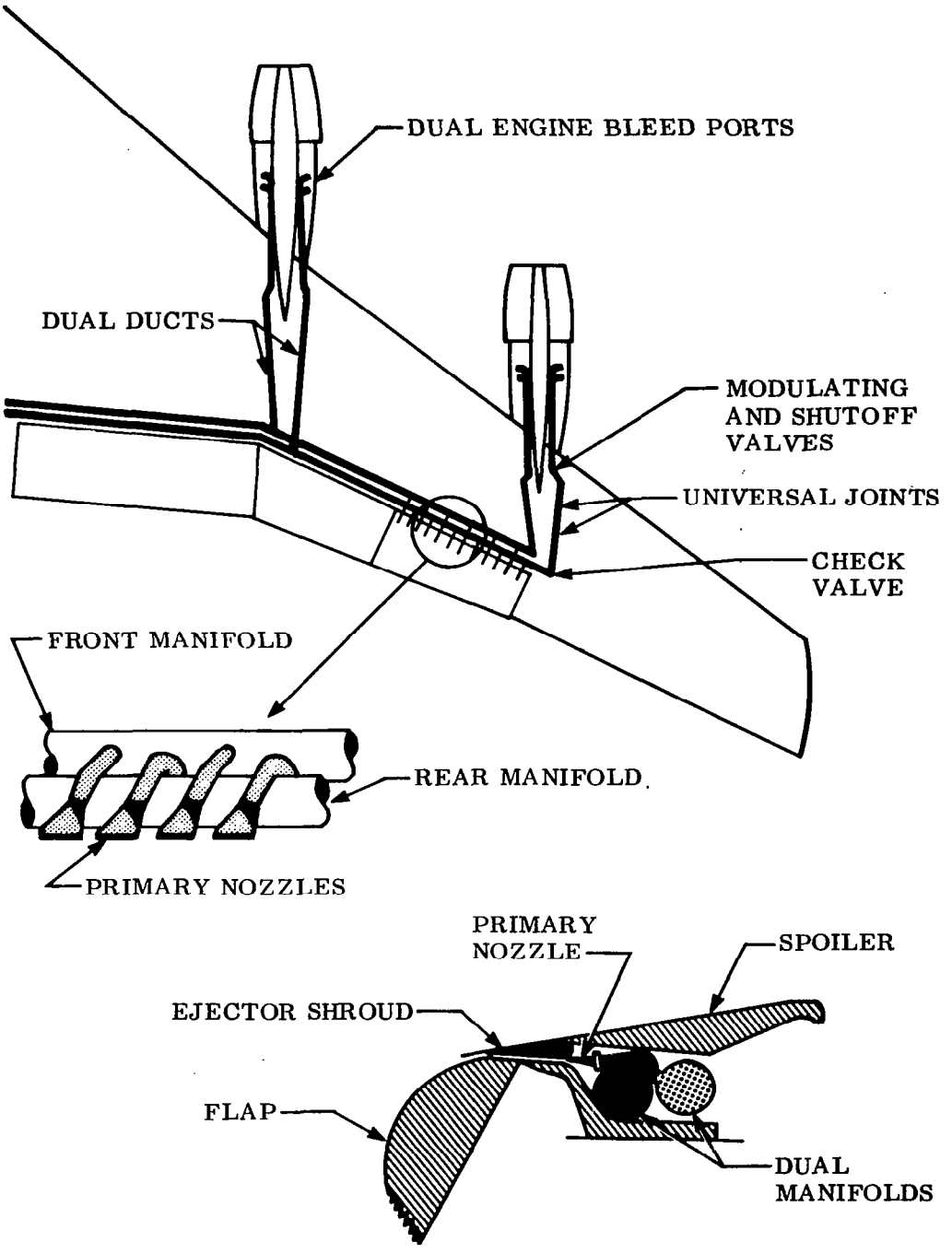

Figure B-2. – Boeing 367-80 Boundary Layer Control System

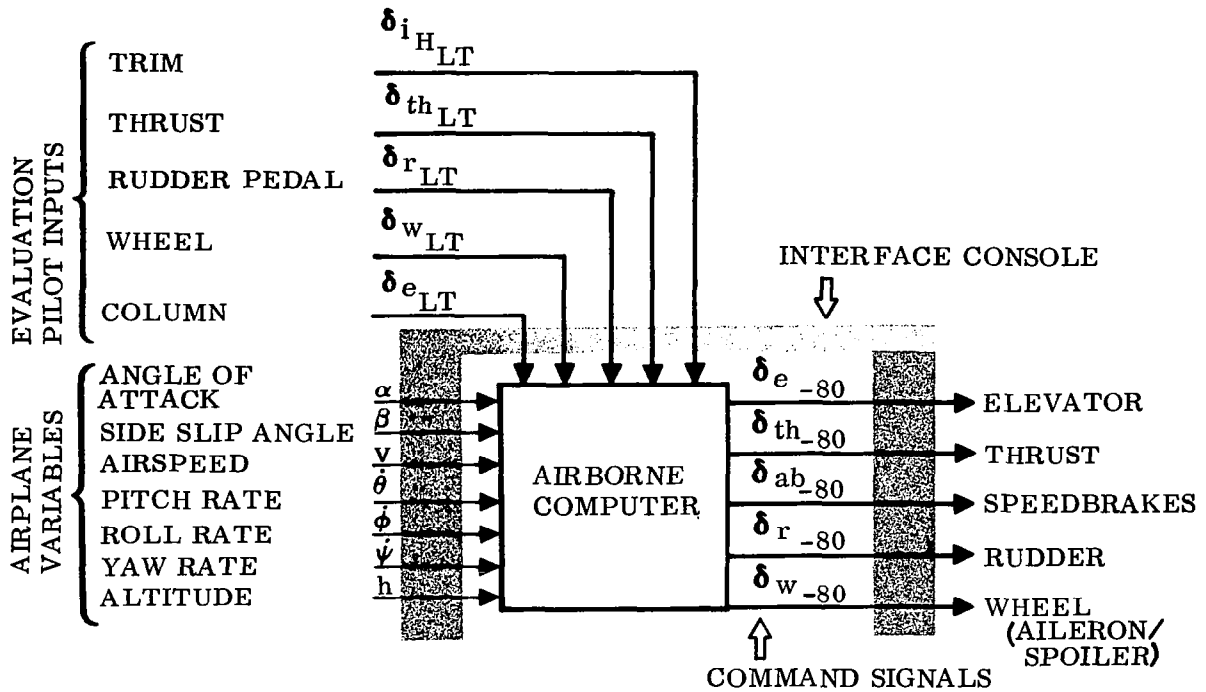

Figure B-3. – Simplified Diagram of the Computation System

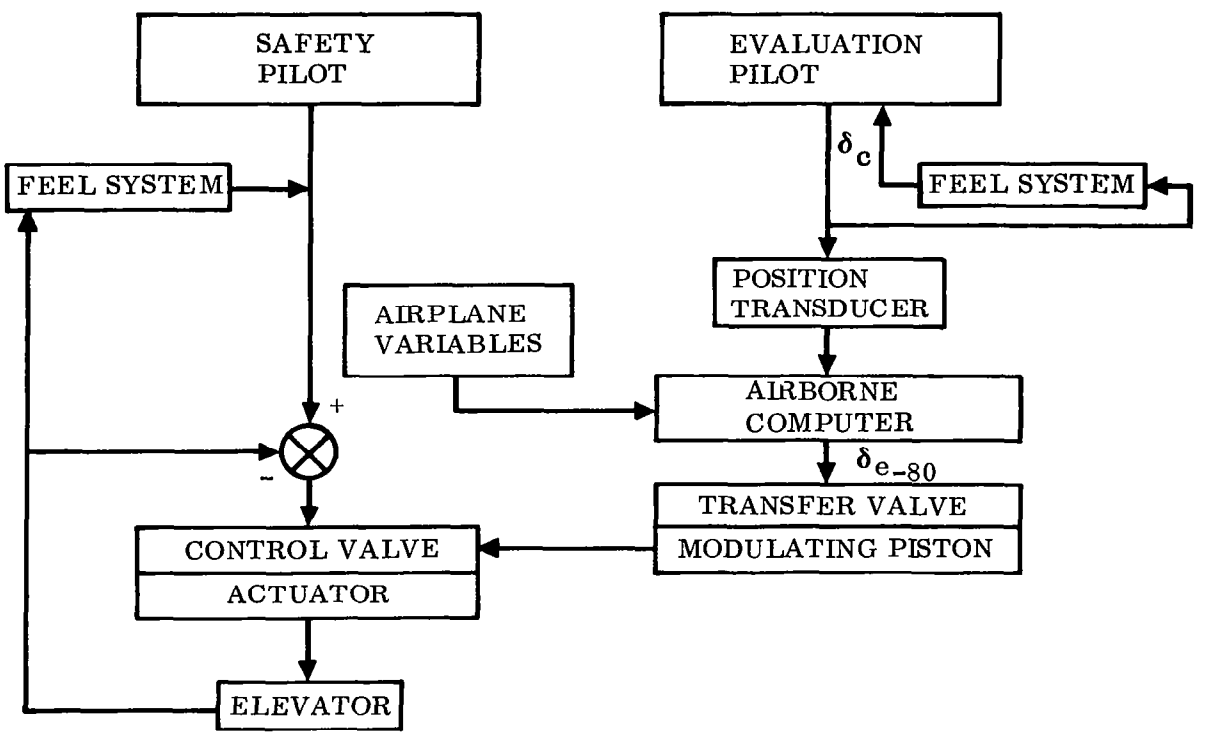

Figure B-4. – Simplified Block Diagram of Elevator System

Noting that the motion variables are, by definition, equal for the 367-80 and the simulated airplane and that $V_{-80} = V_{LT}$, the above equation may be solved for the control variable (δ_e in the pitch case):

$$\delta_{e_{-80}} = \frac{\left(\frac{q_o \, S\bar{c}}{I_{yy}}\right)_{LT}}{\left(\frac{q_o \, S\bar{c}}{I_{yy}}\right)_{-80}} \left\{\frac{1}{C_{M_{\delta_{e_{-80}}}}}\right\} \begin{bmatrix} C_{M_{\delta_{e\,LT}}} & \delta_{e\,LT} \\ C_{M_{\delta_{th\,LT}}} & \delta_{th\,LT} \\ -C_{M_{\delta_{th_{-80}}}} & \delta_{th_{-80}} \\ -C_{M_{\delta_{ab_{-80}}}} & \delta_{ab_{-80}} \\ (C_{M_{\alpha\,LT}} & - C_{M_{\alpha_{-80}}})\Delta\alpha \\ (C_{M_{\dot{\alpha}\,LT}} & - C_{M_{\dot{\alpha}_{-80}}})\alpha \\ (C_{M_{\dot{\theta}\,LT}} & - C_{M_{\dot{\theta}_{-80}}})\dot{\theta} \\ (C_{M_{\Delta V\,LT}} & - C_{M_{\Delta V_{-80}}})\Delta V \end{bmatrix}$$

Similar commands can be derived for the 367-80 rudder, wheel, thrust, and spoiler.

Safety provisions for the inflight simulation are provided both electronically and manually. The electronic equipment contains logic circuits which disengage the simulation should certain limits be exceeded. The evaluation pilot has the capability of disengaging the simulation as does the safety pilot. For any of the above disengagements, control reverts to the safety pilot who has been following all control motions on the normal control system. In the event of a multiple failure, the safety pilot is able to manually override the servo system and fly the aircraft.

Limitations of the Inflight Simulation. — The equations of motion were linearized along with the aerodynamic derivatives by using the small angle assumptions. Any large departure from trim conditions resulted in a degraded simulation due to aerodynamic nonlinearities. As working numbers, limits of ± 10 knots from trim speed, ± 20 degrees of bank angle, ± 10 degrees of sideslip, and ± 0.43 g's were used. The simulation capability of the airplane was limited by accelerations which the controls could produce (the simulation was based on matching center of gravity accelerations). For example, the spoilers operating from a partially deflected setting could produce +0.07 or -0.12 g's.

There was no compensation provided to account for the gross weight change and minor center of gravity variations (± 1.7 percent mac or $M_\alpha = \pm 0.12$ 1/sec^2) due to fuel burnoff.

The response characteristics of the control surfaces affected the accuracy of the simulation. This limitation included the frequency response of the servo system plus any nonlinearities in the linkages, and the effects of airloads. Signal accuracy from the aircraft sensors was important since these signals were fed directly into the computer to form the commands for the control surfaces. Measurement of the significant variables such as angle of attack, sideslip angle, and airspeed was vital to the simulation accuracy. The important sensors were calibrated previously over the flight range used. The aircraft response to a standardized control input provided an overall check of total system response.

The 367-80 simulation system was not designed to produce accurate simulation in a turbulent environment. This factor made it necessary to fly the simulation in relatively calm air (gusts less than ± 1 degree in α or ± 2 degrees in β). Because control positions were a strong function of the aircraft motion variables, gusty conditions would have resulted in errors. These errors would be due primarily to physical separation of the sensor from the actual surface position. For example, a vertical gust first encountered by the nose-boom-mounted angle-of-attack sensor would feed a signal to the spoilers to change the lift and the elevator to correct the pitching moment. A finite time later the gust would reach the wing and later the tail, resulting in a motion which would not be the correct gust response of the simulated airplane.

APPENDIX C

CONFIGURATION DESCRIPTIONS

Tables C-I and C-II present the longitudinal characteristics of the configurations evaluated on the airborne and ground-based simulators, Tables C-III and C-IV present the later characteristics. Representative large transport physical characteristics and aerodynamic coefficients for the base configuration are shown in Table C-V. Characteristics which were not varied significantly during the study are presented in Tables C-V and C-VI.

TABLE C-I

LONGITUDINAL CHARACTERISTICS INFLIGHT SIUMLATION

Inflight Simulation Configuration	L_α 1/sec	M_α $1/sec^2$	$M_{\dot\theta}$ 1/sec	M_{δ_c} $rad/sec^2/in.$	L_{δ_c} rad/sec/in.	$\frac{F_s}{g}$* lb/g	Short Period		Pilot Ratings	
							ω_n rad/sec	ζ	Average	Range
1	0.497	-0.128	-0.587	.0504	-.00635	26	0.650	0.942	4.0	
2	0.521	-0.506	-0.587	.0167	-.00262	128	0.907	0.703	5.5	
3	0.521	-0.506	-0.587	.0252	-.00010	76	0.907	0.703	4.0	
4	0.521	-0.506	-0.587	.0252	-.00164	81	0.907	0.703	3.5	
5	0.521	-0.506	-0.587	.0252	-.00313	83	0.907	0.703	4.5	
6	0.521	-0.506	-0.587	.0504	-.00625	42	0.907	0.703	3.5	
7	0.521	-0.506	-1.174	.0252	-.00316	144	1.071	0.865	4.0	
8	0.552	-1.012	-1.174	.0504	-.00635	91	1.330	0.725	2.75	
9	0.645	-1.398	-0.598	.0625	-.00276	50	1.14	0.525	1.75	1.5 to 2.0

*Windup turn slope at R = 1.0

TABLE C-II

LONGITUDINAL CHARACTERISTICS GROUND-BASED SIMULATOR

Ground-Based Config.	L_α 1/sec	M_α $1/sec^2$	$M_{\dot\theta}$ 1/sec	M_{max} rad/sec^2	M_{δ_c} $rad/sec^2/in.$	L_{δ_c} rad/sec/in.	$\frac{F_s}{g}$* lb/g	Short Period		Pilot Ratings	
								ω_n rad/sec	ζ	Average	Range
1	0.302	0	-0.585	0.166	.0219	-.00195	38	0.420	1.21	5.0	
2	0.302	-0.343	-0.296	0.166	.0219	-.00195	57	0.666	0.580	4.5	
3	0.302	-0.343	-0.585	0.166	.0219	-.00195	78	0.732	0.716	4.0	
4	0.302	-0.506	-0.585	0.166	.0219	-.00195	101	0.834	0.629	4.25	4.0-4.5
5	0.302	-0.735	-0.585	0.166	.0219	-.00195	137	0.957	0.546	6.0	
6	0.302	-0.980	-0.585	0.166	.0219	-.00195	182	1.075	0.485	6.0	
7	0.571	+0.245	-0.585	0.166	.0219	-.00195	25	0.295	2.200	7.5	
8	0.571	0	-0.585	0.107	.0141	-.00195	59	0.575	1.100	5.5	5.5-5.5
9	0.571	0	-0.585	0.166	.0219	-.00195	38	0.575	1.100	4.35	3.5-5.0
10	0.571	0	-0.585	0.166	.0438	-.00391	19	0.575	1.100	5.25	4.75-6.0
11	0.571	0	-0.585	0.213	.0282	-.00195	30	0.575	1.100	4.0	
12	0.571	-0.049	-0.585	0.166	.0438	-.00391	21	0.618	1.045	4.0	
13	0.571	-0.122	-0.585	0.166	.0438	-.00391	23	0.675	0.958	4.5	
14	0.571	-0.122	-0.585	0.245	.0646	-.00391	20	0.675	0.958	4.5	
15	0.571	-0.245	-0.585	0.166	.0219	-.00195	52	0.772	0.843	3.25	3.0-3.5
16	0.571	-0.506	-0.242	0.166	.0219	-.00195	44	0.817	0.605	3.25	
17	0.571	-0.506	-0.585	0.107	.0141	-.00195	112	0.928	0.707	5.25	5.0-5.5
18	0.571	-0.506	-0.585	0.133	.0176	-.00195	88	0.928	0.707	3.75	
19	0.571	-0.506	-0.585	0.166	.0219	+.00195	59	0.928	0.707	2.7	2.5-2.9
20	0.571	-0.506	-0.585	0.166	.0219	0	63	0.928	0.707	2.5	
21	0.571	-0.506	-0.585	0.166	.0219	-.00195	69/89	0.928	0.707	3.4	2.75-4.0
22	0.571	-0.506	-0.585	0.166	.0438	-.00391	34	0.928	0.707	3.3	2.5-4.5
23	0.571	-0.506	-0.585	0.166	.0658	-.00588	30	0.928	0.707	3.25	

*Windup turn slope at n = 1.0

TABLE C-II — Continued

LONGITUDINAL CHARACTERISTICS GROUND-BASED SIMULATOR

Ground-Based Config.	L_α 1/sec	M_α 1/sec^2	$M_{\dot\theta}$ 1/sec	M_{max} rad/sec^2	M_{δ_c} rad/sec^2/in.	L_{δ_c} rad/sec/in.	$\frac{F_s}{g}$* lb/g	Short Period ω_n rad/sec	Short Period ζ	Pilot Ratings Average	Pilot Ratings Range
24	0.571	-0.506	-0.585	0.240	.0316	-.00195	47/60	0.928	0.707	3.1	3.0-3.25
25	0.571	-0.506	-0.585	0.240	.0273	+.00165	62	0.928	0.707	3.25	
26	0.571	-0.506	-0.585	0.245	.0273	0	66	0.928	0.707	3.5	
27	0.571	-0.506	-0.585	0.245	.0646	+.00391	26	0.928	0.707	2.25	2.0-2.5
28	0.571	-0.506	-0.585	0.245	.0646	-.00391	29	0.928	0.707	3.1	3.0-3.25
29	0.571	-0.506	-0.585	0.332	.0439	-.00195	33	0.928	0.707	2.33	2.0-2.5
30	0.571	-0.506	-1.173	0.166	.0219	-.00195	110	1.089	0.865	3.25	
31	0.571	-0.506	-1.173	0.166	.0438	-.00391	55	1.089	0.865	3.25	
32	0.571	-0.506	-1.173	0.245	.0273	-.00165	112	1.089	0.865	3.25	
33	0.571	-0.506	-1.173	0.332	.0439	-.00195	53	1.089	0.865	2.5	
34	0.571	-0.980	-0.585	0.166	.0219	-.00195	102	1.151	0.569	3.25	3.0-3.5
35	0.571	-0.980	-0.585	0.166	.0438	-.00391	51	1.151	0.569	2.0	
36	0.571	-0.980	-0.585	0.245	.0646	-.00391	43	1.151	0.569	2.75	
37	0.571	-0.980	-0.585	0.332	.0439	-.00195	47	1.151	0.569	2.0	
38	0.571	-0.980	-1.173	0.166	.0219	-.00195	148	1.290	0.733	3.5	
39	0.571	-0.980	-1.173	0.166	.0438	-.00391	74	1.290	0.739	3.0	
40	0.571	-0.980	-1.173	0.245	.0438	-.00391	96	1.290	0.739	2.65	2.0-3.25
41	0.571	-1.470	-1.173	0.166	.0219	-.00195	194	1.466	0.645	3.5	
42	0.571	-1.470	-1.173	0.166	.0438	-.00391	97	1.466	0.645	2.5	
43	0.571	-1.470	-1.173	0.332	.0438	-.00195	85	1.466	0.645	3.5	
44	0.925	0.098	-0.585	0.166	.0219	-.00195	35	0.660	1.24	6.5	5.5-7.5
45	0.925	0	-0.245	0.107	.0141	-.00195	25	0.520	1.195	7.1	5.75-8.5
46	0.925	0	-0.585	0.107	.0141	-.00195	60	0.695	1.115	5.75	5.0-6.5
47	0.925	0	-0.585	0.166	.0219	-.00195	38	0.695	1.115	5.0	
48	0.925	-0.122	-0.245	0.166	.0219	-.00195	20	0.635	1.040	4.5	
49	0.925	-0.122	-0.585	0.166	.0219	-.00195	43	0.805	1.000	3.5	3.0-4.0

*Windup turn slope at n = 1.0

TABLE C-II — Concluded

LONGITUDINAL CHARACTERISTICS GROUND-BASED SIMULATOR

Ground-Based Config	L_α 1/sec	M_α $1/sec^2$	$M_{\dot\theta}$ 1/sec	M_{max} rad/sec^2	M_{δ_c} $rad/sec^2/in.$	L_{δ_c} rad/sec/in.	$\frac{F_s}{g}$* lb/g	Short Period		Pilot Ratings	
								ω_n rad/sec	ζ	Average	Range
50	0.925	-0.245	-0.245	0.107	.0141	-.00195	38	0.725	0.920	4.5	
51	0.925	-0.245	-0.585	0.107	.0141	-.00195	74	0.883	0.930	5.0	
52	0.925	-0.245	-0.585	0.166	.0438	-.00391	30	0.883	0.930	3.1	
53	0.925	-0.506	-0.245	0.107	.0141	-.00195	53	0.882	0.762	2.75	
54	0.925	-0.506	-0.585	0.166	.0219	-.00195	56	1.036	0.799	3.5	2.5-4.0
55	0.925	-0.506	-0.585	0.166	.0434	-.00391	28	1.036	0.799	3.1	2.5-3.4
56	0.925	-0.506	-0.585	0.245	.0646	-.00391	24	1.036	0.799	3.0	
57	0.925	-0.980	-0.585	0.166	.0219	-.00195	75	1.242	0.668	3.25	3.0-3.5
58	0.925	-0.980	-0.585	0.166	.0438	-.00391	38	1.242	0.668	2.35	2.0-2.75

*Windup turn slope at n = 1.0

TABLE C-III

LATERAL CHARACTERISTICS INFLIGHT SIMULATION

Inflight Simulation Config	L_{max} rad/sec^2	$\delta_{w_{eff}}$ deg	τ_R sec	t_{max} sec	ϕ_1 deg	ϕ_2 deg	Pilot Rating	
							Average	Range
1	0.150	30	1.14	1.0	1.20	7.25	4.5	
2	0.240	30	1.14	1.0	1.89	10.02	3.4	3.25 to 3.5
3	0.250	50	1.14	1.4	1.40	9.10	4.0	
4	0.267	30	0.60	0.9	1.90	8.95	2.9	2.5 to 3.25
5	0.267	50	1.14	1.0	2.10	12.01	3.75	3.5 to 4.0
6	0.323	30	0.36	0.7	4.00	20.72	2.0	2.0 to 2.0

TABLE C-IV

LATERAL CHARACTERISTICS GROUND-BASED SIMULATION

Ground-Based Config	L_{max} rad/sec^2	$\delta_{w_{eff}}$ deg	τ_R sec	t_{max} sec	ϕ_1 deg	ϕ_2 deg	$\frac{F_w}{\delta_w}$ lb/deg	Pilot Ratings	
								Average	Range
1	.05	30	1.14	0.10	1.0	4.0	0.28	4.0	
2	.05	50	1.14	0.10	1.0	4.0	0.28	5.0	
3	.05	90	1.14	0.10	1.0	4.0	0.28	6.0	
4	0.10	30	1.14	0.20	1.9	6.6	0.28	5.0	
5	0.10	30	1.42	0.10	2.2	6.8	0.28	3.75	
6	0.10	50	1.14	0.20	1.9	6.6	0.28	4.75	4.5 to 5.0
7	0.10	50	1.42	0.10	2.2	6.8	0.28	4.5	
8	0.125	50	1.42	0.10	2.8	9.0	0.28	4.0	
9	0.125	90	1.42	0.10	2.8	9.0	0.28	5.25	
10	0.15	30	1.14	0.10	3.0	12.0	0.28	3.0	
11	0.15	30	1.14	0.20	2.8	10.0	0.19	3.0	2.5 to 3.5
12	0.15	30	1.42	0.10	3.3	10.9	0.28	3.0	
13	0.15	50	0.72	0.20	2.5	8.0	0.28	4.0	
13g	0.15	50	0.72	0.20	2.5	8.0	0.28	7.0*	
14	0.15	50	1.03	0.18	3.0	9.2	0.28	4.0	
15	0.15	50	1.14	0.20	2.8	10.0	0.28	3.7	3.0 to 4.0
15g	0.15	50	1.14	0.20	2.8	10.0	0.28	7.0*	5.5* to 8.5*
16	0.15	50	1.42	0.10	3.3	10.9	0.28	3.6	3.25 to 4.0
17	0.15	50	1.42	0.18	3.1	10.2	0.28	3.5	
18	0.15	50	1.42	0.30	2.7	9.4	0.28	4.0	
19	0.15	50	1.59	0.20	3.1	12.0	0.28	4.5	
20	0.15	75	1.14	0.20	2.8	10.0	0.28	4.3	4.0 to 4.5
21	0.16	50	1.59	0.20	3.3	12.9	0.28	4.35	2.75 to 6.0
21g	0.16	50	1.59	0.20	3.3	12.9	0.28	7.75*	7.0 to 8.5*
22	0.20	50	1.03	0.18	3.9	12.3	0.28	3.4	
23	0.20	50	1.42	0.10	4.4	14.2	0.14	3.0	
24	0.20	50	1.42	0.10	4.4	14.2	0.21	3.1	

*Evaluated with turbulence

TABLE C-IV — Continued

LATERAL CHARACTERISTICS GROUND-BASED SIMULATION

Ground-Based Config	L_{max} rad/sec^2	$\delta_{w_{eff}}$ deg	τ_R sec	t_{max} sec	ϕ_1 deg	ϕ_2 deg	$\frac{F_w}{\delta_w}$ lb/deg	Pilot Ratings	
								Average	Range
25	0.20	50	1.42	0.10	4.4	14.2	0.28	3.35	3.0 to 4.0
26	0.20	50	1.42	0.10	4.4	14.2	0.42	3.9	
27	0.20	50	1.42	0.10	4.4	14.2	0.64	4.1	
28	0.20	90	1.42	0.10	4.4	14.2	0.28	4.0	
29	0.25	30	1.14	0.20	4.8	16.7	0.28	3.0	
29g	0.25	30	1.14	0.20	4.8	16.7	0.28	3.0*	
30	0.25	50	1.14	0	5.3	18.5	0.28	3.5	
31	0.25	50	1.14	0.20	4.8	16.7	0.28	2.75	2.5 to 3.1
31g	0.25	50	1.14	0.20	4.8	16.7	0.28	3.75*	3.5* to 4.0*
32	0.25	50	1.14	0.50	3.5	16.0	0.28	2.75	
33	0.25	50	1.14	0.75	3.2	13.0	0.28	3.3	3.0 to 3.5
34	0.25	50	1.42	0.18	5.2	17.0	0.28	3.0	
35	0.25	50	1.42	0.30	4.6	15.8	0.28	3.5	
36	0.25	75	1.14	0.20	4.8	16.7	0.19	4.0	
36g	0.25	75	1.14	0.20	4.8	16.7	0.19	5.0*	
37	0.267	50	0.60	0.20	4.2	13.3	0.19	3.5	3.0 to 4.0
38	0.28	50	0.72	0.20	4.6	15.1	0.28	2.0	
39	0.30	50	1.03	0.18	5.9	18.6	0.28	2.75	
40	0.30	50	1.14	0.20	5.7	20.1	0.19	3.5*	
41	0.30	50	1.42	0.10	6.5	21.2	0.28	3.4	
42	0.30	75	1.42	0.10	6.5	21.2	0.28	3.5	
43	0.30	90	1.42	0.10	6.5	21.2	0.28	3.5	
44	0.35	50	1.42	0.18	7.2	24.0	0.28	2.5	
45	0.35	50	1.42	0.30	6.2	22.0	0.28	3.0	
46	0.40	50	1.14	0.20	7.5	26.8	0.28	3.5*	
47	0.40	50	1.42	0.10	8.7	28.1	0.28	2.85	2.75 to 3.0
48	0.40	75	1.14	0.20	7.5	26.8	0.28	2.65	2.25 to 3.0

*Evaluated with turbulence

TABLE C-IV — Concluded

LATERAL CHARACTERISTICS GROUND-BASED SIMULATION

Ground-Based Config	L_{max} rad/sec^2	$\delta_{w_{eff}}$ deg	τ_R sec	t_{max} sec	ϕ_1 deg	ϕ_2 deg	$\frac{F_w}{\delta_w}$ lb/deg	Pilot Ratings	
								Average	Range
49	0.40	75	1.42	0.10	8.7	28.1	0.28	3.0	
50	0.40	90	1.42	0.10	8.7	28.1	0.28	2.9	
51	0.43	30	0.60	0.20	6.8	21.0	0.19	1.65	1.5 to 1.75
52	0.47	50	0.60	0.20	7.4	22.8	0.28	3.0	
52g	0.47	50	0.60	0.20	7.4	22.8	0.28	3.1*	3.0* to 3.1*
53	0.47	50	0.72	0.20	7.8	24.4	0.28	3.0	
53g	0.47	50	0.72	0.20	7.8	24.4	0.28	3.5*	
54	0.50	50	1.42	0.10	10.8	35.0	0.28	2.9	
55	0.60	50	1.42	0.10	13.0	42.0	0.28	2.8	
56	0.80	50	1.42	0.10	17.4	56.0	0.28	3.1	
57	0.90	50	1.42	0.10	19.5	63.0	0.28	4.0	
58	1.0	50	1.42	0.10	21.6	70.0	0.28	4.75	

*Evaluated with turbulence

TABLE C-V

LARGE TRANSPORT DESCRIPTION

Physical Characteristics	
Weight	= 500,000 lb
Center of gravity	@ 0.25 mac
Wing area	= 5,500 ft^2
mac	= 28.75 ft
Span	= 215.0 ft
I_{xx}	= 17.5 X 10^6 slug-ft^2
I_{yy}	= 30.0 X 10^6 slug-ft^2
I_{zz}	= 45.0 X 10^6 slug-ft^2
I_{xz}	= 0.95 X 10^6 slug-ft^2
Trim Conditions	
Velocity	= 117.0 knot
	= (197.5 ft/sec)
Angle of attack	= 2.7 degrees
Dynamic pressure	= 46.4 lb/ft^2

TABLE C-VI

SIMULATED LARGE TRANSPORT DYNAMIC CHARACTERISTICS
(BASE CONFIGURATION)

Short period	ω_n = 0.93 rad/sec ζ = 0.71
Phugoid	ω_n = 0.18 rad/sec ζ = 0.14
Dutch roll	ω_n = 0.50 rad/sec ζ = 0.33 ϕ/β = 1.3
Spiral	$t_{1/2}$ = 20 sec
Rolling mode	τ_R = 1.1 sec

TABLE C-VII

LARGE TRANSPORT DESCRIPTION

(BASIC AERODYNAMIC COEFFICIENTS)

DRAG:	C_{D_o}	=	0.45	
	C_{D_α}	=	1.07	/rad
LIFT:	C_{L_o}	=	1.94	
	$C_{L_{\dot\theta}}$	=	0.804	sec/rad
	$C_{L_{\dot\alpha}}$	=	-0.396	sec/rad
	C_{L_α}	=	6.8	/rad
	$C_{L_{\delta_e}}$	=	0.4	/rad
PITCH:	$C_{m_{\dot\alpha}}$	=	-0.555	sec/rad
	$C_{m_{i_H}}$	=	-0.0545	/rad
	C_{m_α}	=	-2.07	/rad
	$C_{m_{\delta_e}}$	=	-2.3	/rad
	$C_{m_{\dot\theta}}$	=	-2.4	sec/rad
ROLL: (unaug.)	C_{l_β}	=	-0.40	/rad
	$C_{l_{\dot\psi}}$	=	0.30	sec/rad
	$C_{l_{\delta_r}}$	=	0.00229	/rad
	$C_{l_{\dot\phi}}$	=	-0.24	sec/rad
	$C_{l_{\delta_w}}$	=	0.10	/rad
YAW: (unaugmented)	C_{n_β}	=	0.18	/rad
	$C_{n_{\dot\phi}}$	=	-0.158	sec/rad
	$C_{n_{\dot\psi}}$	=	-0.267	sec/rad
	$C_{n_{\delta_a}}$	=	0.021	/rad
	$C_{n_{\delta_r}}$	=	-0.120	/rad
SIDE FORCE: (unaugmented)	C_{Y_β}	=	-0.83	/rad
	$C_{Y_{\dot\phi}}$	=	0.57	sec/rad
	$C_{Y_{\dot\psi}}$	=	0.03	sec/rad
	$C_{Y_{\delta_a}}$	=	-0.081	/rad
	$C_{Y_{\delta_r}}$	=	0.246	/rad
AUGMENTATION GAINS:	$\delta_{r/\dot\beta}$	=	-0.30	sec
	$\delta_{r/\dot\phi}$	=	-2.07	sec
	δ_{r/δ_a}	=	0.178	
	$\delta_{a/\dot\psi}$	=	-1.0	sec
	$\delta_{a/\beta}$	=	1.83	

REFERENCES

1. W. M. Eldridge, and H. L. Crane, Use of A Large Jet Transport as an Inflight Dynamic Simulator, (Preprint) 28th Meeting of the AGARD Flight Mechanics Panel, May 1966.

2. D. H. Perry, W. G. A. Port, and J. C. Morrell, A Flight Study of the Side-step Maneuver During Landing, R & M No. 3347, British A. R. C., 1964.

3. Seth B. Anderson, Hervey C. Quigley, and Robert C. Innis, Stability and Control Considerations for STOL Aircraft, (Preprint) No. 65-175, American Institute of Aeronautics and Astronautics, October, 1965.

4. George E. Cooper, "Understanding and Interpreting Pilot Opinion," Aeronautical Engineering Review, Vol. 16, No. 3, March 1957, pp 47-51 and 56.

5. G. A. Patterson and LCDR W. Spangenberg, The Provision of Adequate Lateral Control Power for Landing Approach Conditions, AGARD Report Number 419, January, 1963.

6. W. J. Kehrer: Longitudinal Stability and Control of Large Supersonic Aircraft at Low Speeds, (Preprint) No. 64-586, International Council of the Aeronautical Sciences, August, 1964.

7. L. B. Gratzer and T. J. O'Donnell, "Development of A BLC High-Lift System for High-Speed Airplanes," Journal of Aircraft, Vol. 2, No. 6, November-December 1965, pp 477-484.